

000 001 002 003 004 005 006 007 008 009 010 011 012 013 014 015 016 017 018 019 020 021 022 023 024 025 026 027 028 029 030 031 032 033 034 035 036 037 038 039 040 041 042 043 044 045 046 LENS: MULTI-LEVEL EVALUATION OF MULTIMODAL REAS- SONING WITH LARGE LANGUAGE MODELS

Anonymous authors

Paper under double-blind review

ABSTRACT

Multimodal Large Language Models (MLLMs) have achieved significant advances in integrating visual and linguistic information, yet their ability to reason about complex and real-world scenarios remains limited. Existing benchmarks are usually constructed in a task-oriented manner, without a guarantee that different task samples come from the same data distribution. Therefore, they often fall short in evaluating the synergistic effects of lower-level perceptual capabilities on higher-order reasoning. To lift this limitation, we contribute `Lens`, a multi-level evaluation benchmark of multimodal reasoning with 3.4K contemporary images and 60K+ human-authored questions covering eight tasks and 12 daily scenarios, forming three progressive task tiers, *i.e.*, perception, understanding, and reasoning. One feature is that each image is equipped with rich annotations for all tasks. Thus, this data set intrinsically supports evaluating MLLMs to handle image-invariable prompts, from basic perception to compositional reasoning. In addition, our images have been collected manually from social media, with 53% published after Jan. 2025. We evaluate 15+ frontier MLLMs such as Qwen2.5-VL, InternVL3, GPT-4o and two reasoning models QVQ-Max and Kimi-VL. Most models were released in 2025, and none of them achieve an accuracy beyond 60% in the reasoning tasks. Furthermore, we propose the Self-Driven Multi-Expert Collaborative Framework (SMEC), a framework designed for MLLMs that simulates a panel of experts discussing and exchanging viewpoints via self-generated role-specific prompts. The experimental results confirm the existence of synergistic effects in a hierarchical task structure, where low-level tasks facilitate the reasoning of MLLMs on more complex, high-level tasks. Statistical analysis and ablation studies further demonstrate the comprehensiveness of our dataset and the superiority of our methodology. Our dataset and code will be released upon acceptance.

1 INTRODUCTION

Multimodal Large Language Models (MLLMs) have emerged as a rapidly advancing field in artificial intelligence, demonstrating substantial improvements in visual content recognition and multimodal reasoning (Zhu et al., 2025; Bai et al., 2025; Wu et al., 2024; Team et al., 2024; 2025a). Despite their promising capabilities, MLLMs continue to face significant challenges in interpreting complex and real-world visual environments that are inherently dynamic, diverse, and grounded in physicality. However, existing benchmarks remain limited in their ability to evaluate multi-level reasoning.

Early evaluations were largely based on classical computer vision tasks (Everingham et al., 2010; Lin et al., 2014; Yu et al., 2016) and their integration with natural language. The real-world knowledge was often superficial, resulting in weak alignment between visual input and linguistic output. Secondly, these benchmarks are typically constructed under closed-world assumptions, lacking the inter-task consistency needed to assess reasoning across modalities (Fu et al., 2024; Li et al., 2024a). As a result, the absence of quantitative multi-level evaluation hinders meaningful comparison across MLLMs.

More recent benchmarks have begun to shift toward open-world evaluation and multimodal reasoning tasks (Wu & Xie, 2024; Zang et al., 2025). While this represents progress, current benchmarks do not adequately assess the nuanced performance necessary to evaluate MLLMs’ progression towards human-like intelligence in real-world settings. They require largely primary visual comprehension and fall short of measuring higher-order reasoning and spatial understanding (Yue et al., 2024; Liu et al., 2024c). Furthermore, data distributions often differed between tasks, so that high performance in perceptual tasks did not necessarily translate into strong inference capabilities in more complex integrated multimodal tasks (Fan et al., 2025). As a result, they ignore the synergistic effect of the combinations of lower-order perceptual abilities on higher-order reasoning and are hard to provide a fine-grained assessment.

In this study, we propose a hierarchical and comprehensive evaluation framework `LEnS` specifically designed to assess the multimodal capabilities in real-world scenarios. Our benchmark focuses on both isolated tasks and the integration of perception, understanding, and reasoning—three core tiers essential for intelligent multimodal systems. As shown in Figure 1, `LEnS` encompasses eight tasks, systematically organized into three hierarchical tiers with eight subtasks, and it comprises 3.4K real-world photographs and 60K+ human-authored questions, in 12 diverse scenarios—including streets, stations, schools, homes, and more, which can be roughly divided into three themes: “Home”, “Education”, and “City”, and we visualize the high-frequency words under different themes in Figure 2. 53% of the images are from 2025 and more than 80% of the images are from after September 2024, ensuring the content reflects contemporary environments.

For task design, `LEnS` adopts an open-set configuration, allowing queries to be posed in natural language and grounded in authentic photographic content. This design enables evaluation of model performance in complex, ambiguous, and information-rich settings, better aligning with real-time human demands. Moreover, our benchmark introduces multi-level tasks, which are unified by shared visual contexts, making `LEnS` well-suited for assessing the synergistic effects of lower-level perceptual abilities (*e.g.*, object detection, localization) on higher-order reasoning tasks. To succeed in `LEnS`, models must jointly process multimodal input, recall domain knowledge, and conduct multi-step reasoning to arrive at valid conclusions. Our experimental results confirm that current state-of-the-art MLLMs still struggle with these reasoning-heavy tasks, revealing a significant gap between perception and functional understanding.

To bridge this gap, we propose the Self-Driven Multi-Expert Collaborative Framework (SMEC), a novel reasoning framework that leverages the MLLM itself as a set of specialized experts instantiated through self-generated prompts. Unlike tool-calling approaches (Wang et al., 2025; Gao et al., 2025; Liu et al., 2025b; Zhang et al., 2024b) that rely on external modules, SMEC treats the base MLLM as a versatile reasoning engine: it simulates diverse expert perspectives (*e.g.*, spatial analyst, text interpreter, commonsense reasoner) via role-specific prompts and composes their insights into coherent final answers. This collaborative mechanism encourages the model to extract, expand, and integrate rich, task-relevant information. Our experiments demonstrate that SMEC significantly boosts performance on reasoning tasks within `LEnS`, validating its potential as a general-purpose, language-native method for enhancing multimodal reasoning.

In sum, we make the following contributions:

- **Realistic and Up-to-Date Evaluation.** By leveraging a newly collected set of high-resolution, naturalistic images, our benchmark evaluates the latest multimodal reasoning models in settings that closely reflect real-world complexity.

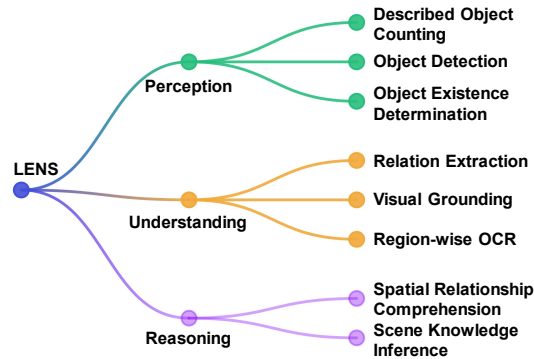


Figure 1: Illustration of the task split in `LEnS`.
Figure 1: Illustration of the task split in `LEnS`. The diagram shows a hierarchical structure with three main levels: Perception, Understanding, and Reasoning, all stemming from a central node labeled `LEnS`. Perception branches into three tasks: Described Object Counting, Object Detection, and Object Existence Determination. Understanding branches into three tasks: Relation Extraction, Visual Grounding, and Region-wise OCR. Reasoning branches into two tasks: Spatial Relationship Comprehension and Scene Knowledge Inference.

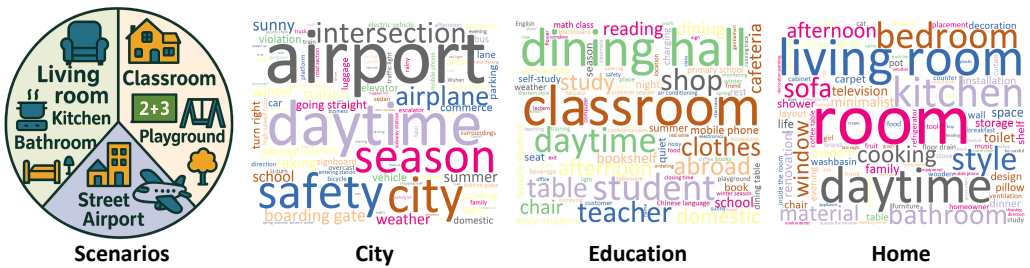


Figure 2: Three core themes, “Education”, “City”, and “Home”, along with their word clouds of the scenario distributions by name size.

- **Multi-Level Evaluation.** It supports fine-grained and interpretable evaluation across three core dimensions—perception, understanding, and reasoning—providing a comprehensive view of a model’s multimodal competence.
- **Synergistic Capability Evaluation.** Unlike existing benchmarks that often assess tasks in isolation, our framework emphasizes the synergistic effects of lower-level perceptual abilities on higher-order reasoning tasks. The experimental results also confirm that low-level tasks facilitate the reasoning of MLLMs on more complex, high-level tasks (*e.g.*, Scene Knowledge Inference).
- **Towards Generalizable Intelligence.** By capturing both perceptual and reasoning performance in integrated tasks, our benchmark helps identify the gaps between current model capabilities and the requirements of human-aligned reasoning systems and measure the shortcomings of current models.
- **Self-driven Reasoning Enhancement.** We introduce SMEC, a self-driven multi-expert collaborative framework that simulates specialized experts within a single MLLM through self-generated prompts. Unlike tool-calling approaches, SMEC enables modular, multi-perspective reasoning natively, leading to significant gains on complex reasoning tasks.

Comparison with existing benchmarks. Compared with existing multimodal benchmarks (Liu et al., 2024c; Yue et al., 2024; Li et al., 2024b), Lens provides more contemporary, diverse, and densely annotated visual content. Our benchmark is constructed from contemporary social-media images, ensuring strong timeliness and significantly reducing the risk of contamination from pre-training corpora. In contrast to task-specific datasets (Liu et al., 2024d;a; Wei et al., 2024), our benchmark provides rich, multi-task annotations with the same visual content, across perception, understanding, and reasoning, enabling controlled analysis of cross-task synergies within a unified distribution. Additionally, Lens offers the detailed thought process in real-world reasoning tasks for potential future research. Appendix A.1 further discusses related work.

2 LENS DATASET AND BENCHMARK

2.1 DATA COLLECTION

The image data collection in our benchmark focuses on real-world scenes to ensure diversity, representativeness, and practicality for visual perception, understanding, and reasoning tasks. To this end, we first defined a set of common real-life scenarios that are highly relevant to typical human visual experiences. The selection principle was that each visual scene should contain distinguishable and representative semantic content. For example, street scenes are usually populated with cars, pedestrians, and storefronts, while indoor environments like classrooms often involve students, teachers, and educational materials. To avoid regional or cultural bias and ensure a broad distribution of content, we collected images from multiple social media platforms, including X (formerly Twitter), Instagram, Weibo, and RedNote. These platforms were chosen due to their global user bases and diverse content coverage across regions and lifestyles. During the collection process, we strictly complied with the copyright and licensing regulations of each platform, ensuring that data was collected only from publicly accessible posts and that no images were downloaded from sources

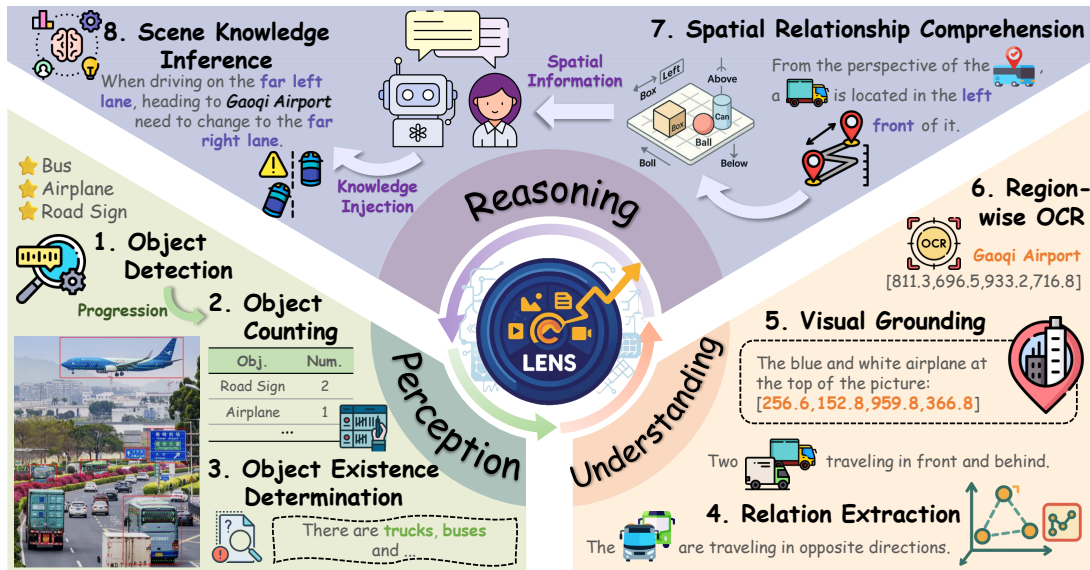


Figure 3: Lens consists of eight tasks at three levels. **Perception** tasks focus on recognizing object attribute and counting. **Understanding** tasks emphasizes localization and inter-object relationships with textual information. **Reasoning** tasks demand the use of external knowledge beyond the visual input and involve multi-step, complex reasoning processes to arrive at the correct answer.

Table 1: Comparison with other recently released multimodal benchmarks.

Benchmarks	Venue	Att.	Cnt	Loc	Rel	Reasoning	Interleaved Image-Text	Image Source
V* (Wu & Xie, 2024)	CVPR'24	✗	✗	✓	✓	✓	✗	SA-1B (Kirillov et al., 2023)
SPEC (Peng et al., 2024)	CVPR'24	✓	✓	✓	✗	✗	✗	Synthesize
MMVP (Tong et al., 2024)	CVPR'24	✓	✗	✗	✗	✗	✗	ImageNet (Russakovsky et al., 2015), LAION-5B (Schuhmann et al., 2022)
HaloQuest (Wang et al., 2024b)	ECCV'24	✓	✗	✗	✓	✓	✗	Open Images (Kuznetsova et al., 2020)
AS-V2 (Wang et al., 2024a)	ECCV'24	✓	✓	✓	✗	✓	✗	COCO (Caesar et al., 2018)
MMBench (Liu et al., 2024c)	ECCV'24	✓	✓	✓	✓	✓	✗	Internet images
HC-RefLoCo (Wei et al., 2024)	NeurIPS'24	✗	✗	✓	✓	✓	✗	Multiple existing datasets
Visual CoT (Shao et al., 2024)	NeurIPS'24	✓	✗	✗	✗	✓	✗	Multiple existing datasets
MC-Bench (Xu et al., 2024)	arXiv'24	✗	✗	✓	✗	✓	✓	Multiple existing datasets, Internet
CODE (Zang et al., 2025)	IJCV'25	✓	✓	✓	✗	✗	✗	Flickr30k series (Young et al., 2014; Plummer et al., 2015)
ChatterBox (Tian et al., 2025)	AAAI'25	✓	✓	✓	✗	✓	✗	Visual Genome (Krishna et al., 2017)
Lens	-	✓	✓	✓	✓	✓	✓	Collect manually from social media 53% published later than Jan. 2025

"Att.": Attribute; "Cnt": Count; "Loc": Localization; "Rel": Relation

explicitly prohibiting data reuse or redistribution. Moreover, to facilitate the evaluation of multiple subtasks within the same image (e.g., detection, OCR, scene knowledge inference), we curated images that exhibit rich semantic content while maintaining scene clarity. Complex or ambiguous images were manually filtered out to avoid introducing noise that could hinder benchmarking or evaluation consistency. Please note that we manually collect these data that are completely open to the Internet and have complied with the developer agreement of the relevant platform (e.g., Developer Policy of X¹ and Meta²), ensuring non-commercial use, erasing geographic information, user personal information, etc. from the original data. Images containing sensitive personal information were either excluded or processed to blur or mask sensitive regions, to mitigate privacy risks. For further details, please refer to the appendix A.4.

¹<https://developer.x.com/en/use-cases/do-research/academic-research>

²<https://developers.facebook.com/docs/instagram-platform>

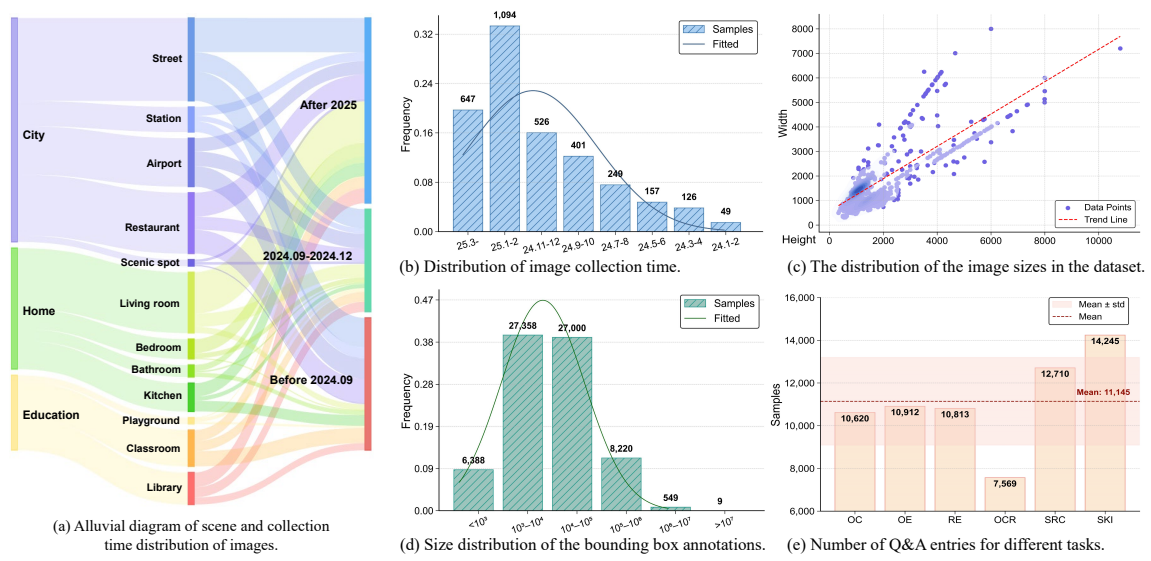


Figure 4: Statistical analysis of our dataset. We visualize the temporal distribution of the images for different scenarios, size distribution of images and bounding box annotations, and number of QA entries for different tasks, demonstrating the timeliness and diversity of our data.

2.2 TASK DESIGN AND ANNOTATION PROCESS

To construct a comprehensive and diverse benchmark, we recruited over 50 undergraduate and graduate students (including authors) as human annotators to assist in the process of question collection and task annotation and paid the corresponding salary. These annotators were carefully trained to ensure high annotation quality and consistency. As shown in Figure 3, the generated questions were divided into three major categories: Perception, Understanding, and Reasoning. For Perception and Understanding, they primarily target the model’s ability to perceive visual objects and align them accurately with natural language descriptions. They emphasize fine-grained visual grounding and object recognition rather than abstract reasoning. At last, reasoning-based questions aim to evaluate the model’s ability to understand user intent and reason based on external knowledge, commonsense, physical laws, or background information beyond the purely visual content of the image. Based on these assessment dimensions, we compare `Lens` with related multimodal benchmarks in Table 1 and formulate our challenging open-ended, language-driven tasks: Object Counting (OC), Object Detection (OD), Object Existence Determination (OE), Relation Extraction (RE), Visual Grounding (VG), Region-wise OCR (OCR), Spatial Relationship Comprehension (SRC), and Scene Knowledge Inference (SKI). We provide a more detailed introduction of these tasks in Appendix A.2.

2.3 DATA ANALYSIS

We aim to construct a dataset that is not only comprehensive and dynamic but also emphasizes reasoning ability practices. In the following analysis, we demonstrate the strengths of our benchmark in terms of diversity of images and annotations. The quantitative results are visualized in Figure 4.

First, our benchmark incorporates scene-aware content and real-time data. As shown in Figure 4, more than 50% of the images in our dataset were collected in 2025, and approximately 70% were collected in November 2024 and beyond, which avoids potential data leakage. Many images reflect dynamic scenes (e.g., crowded streets, interactive environments) captured at different times and locations, aligning with real-world scenarios.

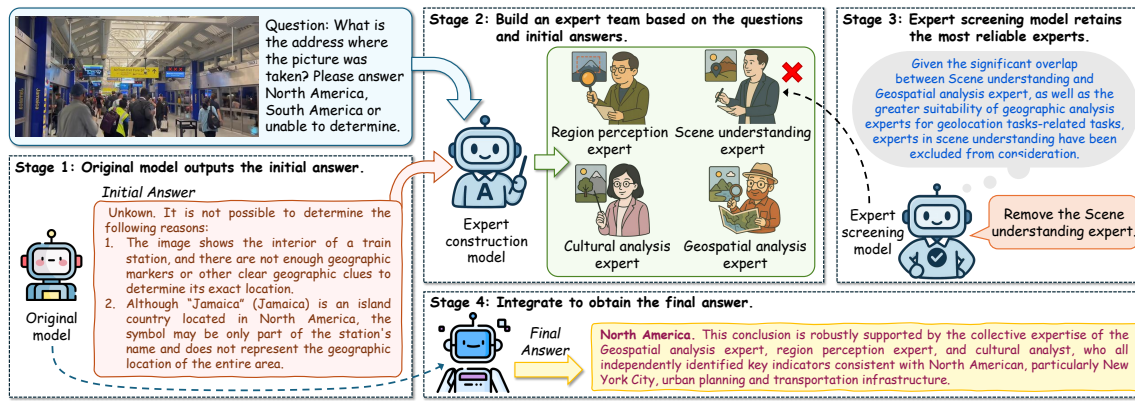


Figure 5: SMEC is a step-wise reasoning framework for answering complex visual questions using the Multi-Expert Collaboration. Starting from an initial model response, SMEC constructs a specialized expert team, to re-evaluate and refine the answer. Through expert screening and integration, unreliable and duplicated experts are filtered out, and a consensus-based final answer is produced, demonstrating the advantages of modular, expert-driven collaboration in visual reasoning tasks.

Second, in our dataset, the coverage of a wide range of object categories, scene types, and bounding box annotations further supports diverse downstream tasks from detection to high-level semantic inference and interleaved image-text understanding. As illustrated in Figure 4 (c), the high resolution of the images in our dataset makes it challenging for fine-grained understanding of the model and supports evaluation across varying input sizes. Additionally, as shown in Figure 4 (d), the various objects are labeled with different sizes of bounding boxes to meet the needs of multi-scale object detection and region-wise OCR evaluation.

Furthermore, beyond perception, our dataset facilitates reasoning-oriented research by supporting tasks that require: Spatial reasoning (*e.g.*, understanding object layouts and geometric relationships). Relational inference (*e.g.*, extracting interactions between objects). Commonsense knowledge application (*e.g.*, inferring the feasibility of a behavior or scene functionalities). Cross-modal alignment (*e.g.*, grounding free-form language to specific visual content). We also analyze the question-answer pairs distribution of these tasks and Figure 4 (e) shows that over 60% of the questions in the dataset go beyond simple recognition, explicitly encouraging models to reason about the scene, context, and user intent. Please refer to the Appendix A.5 for more low-level visual analysis.

3 SELF-DRIVEN MULTI-EXPERT COLLABORATIVE FRAMEWORK

We propose a Self-Driven Multi-Expert Collaborative Framework to tackle complex visual reasoning tasks that require diverse domain expertise and multi-level inference. Built on an instruction-tuned MLLM, our framework dynamically assembles a set of self-generated experts, each embodying a distinct reasoning perspective, as shown in Figure 5.

Expert Generation via Prompted Role Construction. Given a query q , the base model θ first produces a coarse initial answer a_0 . To enrich the reasoning space, a Meta Generation Prompt p_g is used to iteratively generate expert role descriptions d_q^t , simulating specialized agents (*e.g.*, geospatial analyst, cultural analyst). Each valid description yields a new expert response a_t , which is added to the answer set A . This loop continues until either a diversity criterion is violated or a maximum number of iterations N_t is reached.

Prompt Adaptation and Redundancy Filtering. To avoid degenerate expert generation, the framework dynamically updates p_g when semantically redundant descriptions emerge. This adaptation encourages

282 exploration of novel expert roles. Implicit expert screening is performed by discarding repetitive or low-
 283 information descriptions, ensuring a concise yet diverse expert team with minimal computational overhead.
 284

285 **Consensus-Driven Answer Integration.** The final stage aggregates the expert responses via a Collaboration
 286 Prompt p_c , prompting θ to synthesize a unified answer a_{final} through deliberative reasoning. This mimics
 287 human expert panels that reconcile differing views to reach a robust consensus.

288 We detail a formal description of the process in Appendix A.10. By this way, our framework instantiates
 289 modular experts purely via prompt-based self-conditioning. Unlike fixed-rule multi-agent systems and
 290 tool-calling methods, our framework leverages the generative flexibility of MLLM to dynamically instantiate
 291 and evolve its behaviors, without requiring external task-specific supervision.

292 4 EXPERIMENTS

293 4.1 EVALUATION MODELS

294 To illustrate the difficulty of our benchmark and evaluate the latest advances in current research, we evaluate
 295 various MLLMs belonging to three major categories: Closed-source generalist MLLMs, such as GPT-4o
 296 (Achiam et al., 2023) and Gemini2.5 Pro (Team et al., 2024). Open-source generalist MLLMs like Qwen2.5-
 297 VL (Bai et al., 2025), Deepseek-VL2 (Wu et al., 2024), Gemma3 (Team et al., 2025a), InternVL3 (Zhu et al.,
 298 2025). Multimodal reasoning models QvQ-Max, Kimi-VL-thinking (Team et al., 2025b) and GLM-4.1V-
 299 Thinking (Hong et al., 2025), focusing on advanced reasoning capabilities. The release dates of these models
 300 are distributed from Dec. 2024 to Apr. 2025.

301 4.2 EVALUATION STRATEGY

302 To ensure a fair and efficient assessment of model performance across our benchmark, we adopt two evaluation
 303 strategies for main results. For perception and understanding tasks, models were evaluated based on their
 304 direct outputs without additional inference-time computations. For complex reasoning tasks, which require
 305 deeper multi-step inference, we allow models to generate multiple candidate responses per question and
 306 the final prediction is then selected via majority voting (Liu et al., 2025a). For qualitative judgment, we
 307 follow prior work (Wang et al., 2023) and employ a large language model (*e.g.*, GLM4-flash (GLM et al.,
 308 2024)) as an automatic evaluator. The LLM is prompted to produce multiple pieces of evaluation evidence for
 309 calibration, comparing the model-generated responses against human-annotated answers, aiming to offer a
 310 consistent framework for evaluating model performance across diverse tasks.

311 4.3 EVALUATION RESULTS

312 We evaluate a suite of state-of-the-art Multimodal Large Language Models on our benchmark, which spans
 313 three tiers and eight tasks. Results, as shown in Table 2, reveal insights into model scaling, inter-task
 314 dependencies, and capability gaps in current MLLMs.

315 **Model Scaling and General Trends.** We observe a consistent performance gain with increased model size
 316 in both closed- and open-source models. For example, Qwen2.5-VL improves steadily from 3B to 72B,
 317 achieving top performance on reasoning tasks. InternVL3 shows similar gains in OD, rising from 18.39%
 318 (2B) to 47.44% (78B), though performance saturates at higher scales. These trends confirm that scaling
 319 remains a key driver for multimodal reasoning, albeit with diminishing returns in some subtasks.

320 **Perception: Foundation for Higher Cognition.** Perception-level tasks form the backbone of visual reasoning.
 321 Closed-source models like Gemini2.5-Pro and GPT-4o excel at OE (86.59% and 85.09%, respectively),
 322 although OD support is lacking. Among open-source models, Deepseek-VL2 and Qwen2.5-VL-72B deliver

329 Table 2: Comparison of state-of-the-art methods on `Lens`. We evaluate object detection (OD) performance
 330 using AP₅₀ (Lin et al., 2014), visual grounding (VG) performance with ACC@0.5 (Xiao et al., 2024), and use
 331 accuracy for other tasks. Task abbreviations follow the definitions provided in Section 2.2. “MoE 1B/3B”
 332 denotes 3B Mixture of Experts model with 1B parameters activated. “N/A” denotes the official documentation
 333 does not confirm that the model is applicable for the task. Best performing models are shaded in red.

Methods	Model size	Perception			Understanding			Reasoning	
		OC	OD	OE	RE	VG	OCR	SRC	SKI
MLLM (closed source)									
⌚ GPT-4o	-	54.32	N/A	85.09	72.77	N/A	42.86	51.14	55.20
◆ Gemini2.5-Pro	-	60.18	47.40	86.59	76.52	25.61	61.95	56.20	59.31
Open source									
⌚ Deepseek-VL2-tiny	MoE 1B/3B	56.22	21.12	72.11	58.73	16.09	44.01	38.97	45.12
⌚ Deepseek-VL2	MoE 4.5B/27B	61.41	46.08	77.68	69.18	42.47	48.76	44.58	49.50
⌚ Gemma3	4B	38.85	N/A	71.88	62.98	N/A	27.03	39.53	45.18
⌚ Gemma3	12B	44.65	N/A	73.21	62.78	N/A	33.98	43.33	48.56
⌚ InternVL3	2B	55.81	18.39	71.96	64.49	15.22	45.51	40.56	48.59
⌚ InternVL3	9B	55.63	25.79	77.49	67.18	18.18	48.79	44.69	51.32
⌚ InternVL3	38B	62.78	43.44	81.60	71.37	24.98	51.72	47.18	51.85
⌚ InternVL3	78B	61.38	47.44	84.87	74.93	27.24	54.21	49.39	55.17
⌚ Qwen2.5-VL	3B	58.76	35.16	74.01	66.52	39.44	52.43	40.33	46.50
⌚ Qwen2.5-VL	7B	58.35	37.75	83.75	71.58	40.11	61.65	46.28	48.87
⌚ Qwen2.5-VL	32B	62.25	39.93	83.60	74.57	41.15	65.64	51.66	51.54
⌚ Qwen2.5-VL	72B	59.75	43.48	85.67	75.98	44.98	68.51	53.65	54.79
Reasoning model									
⌚ QVQ-Max	72B	49.95	N/A	85.37	74.01	N/A	58.67	50.80	58.86
⌚ Kimi-VL-thinking	MoE 2.8B/16B	46.87	N/A	72.77	48.16	N/A	30.21	29.40	36.44

356 competitive OD and OC performance. Notably, models with stronger perception capabilities tend to exhibit
 357 superior reasoning performance, highlighting the foundational role of low-level visual understanding.

358 **Understanding: Progress and Bottlenecks.** Understanding tasks assess models’ ability to interpret structured
 359 visual semantics with textual information. Gemini2.5-Pro leads in RE (76.52%) and OCR (61.95%),
 360 showcasing robust relational and textual grounding. However, VG remains a bottleneck even for large-scale
 361 models like InternVL3-78B (27.24%) and Qwen2.5-VL-72B (44.98%), suggesting persistent challenges in
 362 fine-grained spatial-semantic alignment.

363 **Reasoning: High-Level Generalization.** Reasoning tasks are the most demanding. Closed-source models
 364 such as GPT-4o and Gemini2.5-Pro achieve strong results (51.14%/56.20% on SRC and 55.20%/59.31%
 365 on SKI). Among open-source models, Qwen2.5-VL-72B leads, while the reasoning-specialized QVQ-Max
 366 approaches closed-source performance (58.86% on SKI) despite lacking OD and VG capabilities. This
 367 suggests that explicit reasoning models can partially compensate for perceptual limitations, likely relying on
 368 test-time scaling rather than grounded perception.

370 4.4 SYNERGISTIC EFFECTS ANALYSIS

371 To analyze the cross-task performance patterns of different models, we perform a statistical analysis of the
 372 synergies between different tasks and visualized the results as in Figure 6. We compute the Pearson correlation
 373 coefficients between Perception and Understanding tasks and observe notable interdependencies. OC and RE
 374 exhibit a strong positive correlation of 0.73, while OE and OCR show a similarly significant correlation of
 375 0.67. These results indicate that effective performance in perception directly contributes to understanding,

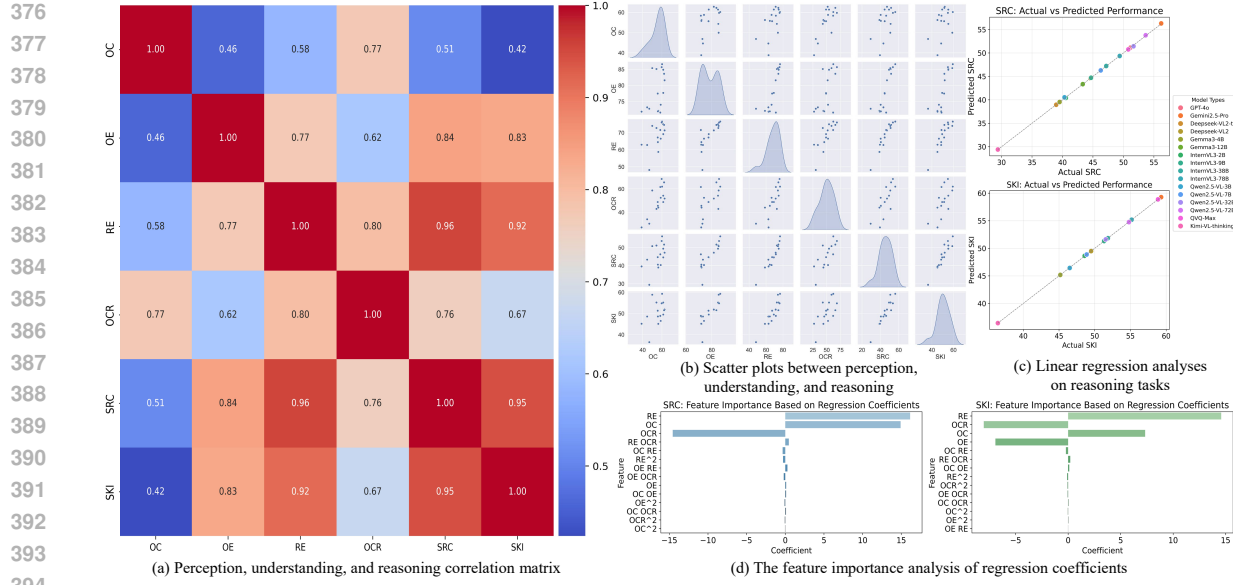


Figure 6: Statistical analysis of model accuracy and synergies between different tasks.

which in turn underpins downstream reasoning. Scatter plot visualizations further confirm these links, OCR, in particular, correlates strongly with both SRC and SKI, underscoring its central role in enabling semantic reasoning. Linear regression analyses reinforce these findings: OE and OCR are strong predictors of SRC, while OC and RE significantly influence SKI, highlighting how object-level detection and relational reasoning jointly support high-level inference. Finally, we apply second-order polynomial regression and the feature importance analysis of regression coefficients reveals task-specific contributions. These insights collectively demonstrate the layered structure of visual reasoning pipelines, where perception and understanding stages must be well-aligned to support robust inference. For further analysis, please refer to the appendix A.7.

4.5 EFFECTIVENESS OF SMEC

To further evaluate the effectiveness of our proposed SMEC framework, we conduct experiments on the Scene Knowledge Inference (SKI) task using both a sampled subset of 3,500 question–answer pairs and the full test set (Table 3). Compared to the direct inference baseline, SMEC consistently improves performance across both model scales and different iteration depths. For Qwen2.5VL-7B, accuracy increases from 39.80% to 43.24% as the number of iterations N_t grows from 1 to 3, demonstrating the benefits of multi-step expert collaboration. Notably, SMEC also outperforms Self-Refine (Madaan et al., 2023) and Majority voting (Chen et al., 2024b) under the same setting. A similar trend appears at larger scales. With Qwen2.5VL-32B, SMEC improves accuracy from 49.17% to 52.44% with three iterations, confirming that the benefits of iterative expert collaboration scale with model capacity. Importantly, when evaluated on the full test set rather than the 3,500-sample subset, SMEC continues to provide consistent improvements (+3.12%). This indicates that SMEC’s gains are not distribution-specific and remain stable under more comprehensive evaluation conditions.

Table 3: Accuracy comparison with different settings.

Methods	Model	Iterations	Performance
Direct	Qwen2.5VL-7b	-	39.80
Majority voting	Qwen2.5VL-7b	-	40.66
Self-Refine	Qwen2.5VL-7b	-	40.51 (+0.71)
SMEC	Qwen2.5VL-7b	1	41.35 (+1.55)
SMEC	Qwen2.5VL-7b	2	42.97 (+3.17)
SMEC	Qwen2.5VL-7b	3	43.24 (+3.44)
Direct	Qwen2.5VL-32b	-	49.17
SMEC	Qwen2.5VL-32b	3	52.44 (+3.27)
Direct (Full data)	Qwen2.5VL-32b	-	51.54
SMEC (Full data)	Qwen2.5VL-32b	3	54.66 (+3.12)

423

5 CONCLUSION

425 We contribute `Lens`, a multi-level benchmark designed to evaluate Multimodal Large Language Models
 426 (MLLMs) across perception, understanding, and reasoning. Unlike prior benchmarks, `Lens` aligns all tasks
 427 to the same set of realistic, contemporary images, enabling fine-grained analysis of how low-level visual
 428 capabilities support higher-order reasoning. The evaluation of recent MLLMs further reveals a consistent
 429 performance gap in reasoning tasks, highlighting the limitations of current models in integrating perception
 430 and cognition. To address this, we proposed SMEC, a self-driven multi-expert collaborative framework
 431 that prompts the MLLM to simulate a panel of specialized agents. Together, `Lens` and SMEC offer a new
 432 paradigm for evaluating and enhancing reasoning intelligence in MLLMs, paving the way to more robust,
 433 human-aligned multimodal intelligence.

434

6 ETHICS STATEMENT

435 **Data Collection and Privacy.** All images in the `Lens` dataset were collected manually from publicly
 436 available posts on social media platforms, including X (formerly Twitter), Instagram, Weibo, and RedNote.
 437 We strictly complied with the developer agreements and copyright/licensing regulations of these platforms.
 438 No private or restricted data was accessed, and all collection adhered to academic research policies.

439 **Human Annotation.** The dataset was constructed with the assistance of more than 50 undergraduate and
 440 graduate student annotators, who were trained to ensure annotation quality and consistency. All annotators
 441 were fairly compensated for their work. The annotation process involved only task-related labeling
 442 (*e.g.*, bounding boxes, question-answer generation) and did not involve collection of personal or sensitive
 443 information about the annotators.

444 **Bias, Fairness, and Representation.** Although images were sourced from global platforms to ensure diversity
 445 of cultural and regional content, dataset bias may still exist due to platform-level demographic imbalances
 446 and uneven scenario representation. We acknowledge that these limitations may influence model evaluation
 447 results, and we encourage future work to further broaden geographic and cultural coverage.

448 **Research Integrity and Transparency.** This study follows established standards of research integrity. We
 449 provide detailed dataset descriptions, evaluation protocols, and implementation details. We have no conflicts
 450 of interest or external sponsorship that might bias the study.

451

7 REPRODUCIBILITY STATEMENT

452 We have taken extensive measures to ensure the reproducibility of our results. A complete description of the
 453 `Lens` dataset, including data collection principles, filtering steps, and annotation procedures, is provided in
 454 Section 2 and Appendix. Details of the evaluation tasks, metrics, and benchmark comparisons are reported in
 455 Section 4, with additional analyses in Appendix. The implementation of our proposed Self-Driven Multi-
 456 Expert Collaborative Framework (SMEC), including the expert construction, screening, and integration
 457 process, is fully described in Section 3 and formalized in Appendix A.9. Hyperparameter settings, model
 458 configurations, and ablation experiments are included in the appendix to facilitate replication of results.
 459 Together, these resources ensure that both dataset construction and methodological contributions can be
 460 faithfully reproduced by the research community.

461

REFERENCES

462 Josh Achiam, Steven Adler, Sandhini Agarwal, Lama Ahmad, Ilge Akkaya, Florencia Leoni Aleman, Diogo
 463 Almeida, Janko Altenschmidt, Sam Altman, Shyamal Anadkat, et al. Gpt-4 technical report. *arXiv preprint*

470 *arXiv:2303.08774*, 2023.

471

472 Jean-Baptiste Alayrac, Jeff Donahue, Pauline Luc, Antoine Miech, Iain Barr, Yana Hasson, Karel Lenc,
 473 Arthur Mensch, Katherine Millican, Malcolm Reynolds, et al. Flamingo: a visual language model for
 474 few-shot learning. *Advances in neural information processing systems*, 35:23716–23736, 2022.

475

476 Alisson Azzolini, Junjie Bai, Hannah Brandon, Jiaxin Cao, Prithvijit Chattopadhyay, Huayu Chen, Jinju Chu,
 477 Yin Cui, Jenna Diamond, Yifan Ding, et al. Cosmos-reason1: From physical common sense to embodied
 478 reasoning. *arXiv preprint arXiv:2503.15558*, 2025.

479

480 Shuai Bai, Keqin Chen, Xuejing Liu, Jialin Wang, Wenbin Ge, Sibo Song, Kai Dang, Peng Wang, Shijie
 481 Wang, Jun Tang, et al. Qwen2. 5-vl technical report. *arXiv preprint arXiv:2502.13923*, 2025.

482

483 Holger Caesar, Jasper Uijlings, and Vittorio Ferrari. Coco-stuff: Thing and stuff classes in context. In
 484 *Proceedings of the IEEE conference on computer vision and pattern recognition*, pp. 1209–1218, 2018.

485

486 Guangyao Chen, Siwei Dong, Yu Shu, Ge Zhang, Jaward Sesay, Börje F Karlsson, Jie Fu, and Yemin Shi.
 487 Autoagents: A framework for automatic agent generation. *arXiv preprint arXiv:2309.17288*, 2023a.

488

489 Jiangjie Chen, Xintao Wang, Rui Xu, Siyu Yuan, Yikai Zhang, Wei Shi, Jian Xie, Shuang Li, Ruihan Yang,
 490 Tinghui Zhu, et al. From persona to personalization: A survey on role-playing language agents. *arXiv
 491 preprint arXiv:2404.18231*, 2024a.

492

493 Keqin Chen, Zhao Zhang, Weili Zeng, Richong Zhang, Feng Zhu, and Rui Zhao. Shikra: Unleashing
 494 multimodal llm’s referential dialogue magic. *arXiv preprint arXiv:2306.15195*, 2023b.

495

496 Lingjiao Chen, Jared Quincy Davis, Boris Hanin, Peter Bailis, Ion Stoica, Matei A Zaharia, and James Y
 497 Zou. Are more llm calls all you need? towards the scaling properties of compound ai systems. *Advances in
 498 Neural Information Processing Systems*, 37:45767–45790, 2024b.

499

500 Wei Chen, Long Chen, and Yu Wu. An efficient and effective transformer decoder-based framework for
 501 multi-task visual grounding. In *European Conference on Computer Vision*, pp. 125–141, 2024c.

502

503 Weize Chen, Yusheng Su, Jingwei Zuo, Cheng Yang, Chenfei Yuan, Chi-Min Chan, Heyang Yu, Yaxi Lu,
 504 Yi-Hsin Hung, Chen Qian, et al. Agentverse: Facilitating multi-agent collaboration and exploring emergent
 505 behaviors. In *The Twelfth International Conference on Learning Representations*, 2023c.

506

507 Zebang Cheng, Zhi-Qi Cheng, Jun-Yan He, Kai Wang, Yuxiang Lin, Zheng Lian, Xiaojiang Peng, and
 508 Alexander Hauptmann. Emotion-llama: Multimodal emotion recognition and reasoning with instruction
 509 tuning. *Advances in Neural Information Processing Systems*, 37:110805–110853, 2024.

510

511 Ming Dai, Lingfeng Yang, Yihao Xu, Zhenhua Feng, and Wankou Yang. Simvg: A simple framework for
 512 visual grounding with decoupled multi-modal fusion. *Advances in neural information processing systems*,
 513 37:121670–121698, 2024.

514

515 Jiajun Deng, Zhengyuan Yang, Tianlang Chen, Wengang Zhou, and Houqiang Li. Transvg: End-to-end visual
 516 grounding with transformers. In *Proceedings of the IEEE/CVF International Conference on Computer
 517 Vision*, pp. 1769–1779, 2021.

518

519 Qingxiu Dong, Lei Li, Damai Dai, Ce Zheng, Jingyuan Ma, Rui Li, Heming Xia, Jingjing Xu, Zhiyong Wu,
 520 Tianyu Liu, et al. A survey on in-context learning. *arXiv preprint arXiv:2301.00234*, 2022.

521

522 Mark Everingham, Luc Van Gool, Christopher KI Williams, John Winn, and Andrew Zisserman. The pascal
 523 visual object classes (voc) challenge. *International journal of computer vision*, 88:303–338, 2010.

517 David Fan, Shengbang Tong, Jiachen Zhu, Koustuv Sinha, Zhuang Liu, Xinlei Chen, Michael Rabbat, Nicolas
 518 Ballas, Yann LeCun, Amir Bar, et al. Scaling language-free visual representation learning. *arXiv preprint*
 519 *arXiv:2504.01017*, 2025.

520

521 Chaoyou Fu, Yi-Fan Zhang, Shukang Yin, Bo Li, Xinyu Fang, Sirui Zhao, Haodong Duan, Xing Sun, Ziwei
 522 Liu, Liang Wang, et al. Mme-survey: A comprehensive survey on evaluation of multimodal llms. *arXiv*
 523 *preprint arXiv:2411.15296*, 2024.

524

525 Zhi Gao, Bofei Zhang, Pengxiang Li, Xiaojian Ma, Tao Yuan, Yue Fan, Yuwei Wu, Yunde Jia, Song-
 526 Chun Zhu, and Qing Li. Multi-modal agent tuning: Building a VLM-driven agent for efficient tool
 527 usage. In *The Thirteenth International Conference on Learning Representations*, 2025. URL <https://openreview.net/forum?id=0bmGL4q7vJ>.

528

529 Team GLM, Aohan Zeng, Bin Xu, Bowen Wang, Chenhui Zhang, Da Yin, Dan Zhang, Diego Rojas, Guanyu
 530 Feng, Hanlin Zhao, et al. Chatglm: A family of large language models from glm-130b to glm-4 all tools.
 531 *arXiv preprint arXiv:2406.12793*, 2024.

532

533 Daya Guo, Dejian Yang, Huawei Zhang, Junxiao Song, Ruoyu Zhang, Runxin Xu, Qihao Zhu, Shirong Ma,
 534 Peiyi Wang, Xiao Bi, et al. Deepseek-r1: Incentivizing reasoning capability in llms via reinforcement
 535 learning. *arXiv preprint arXiv:2501.12948*, 2025.

536

537 Tanmay Gupta and Aniruddha Kembhavi. Visual programming: Compositional visual reasoning without
 538 training. In *Proceedings of the IEEE/CVF conference on computer vision and pattern recognition*, pp.
 539 14953–14962, 2023.

540

541 Sirui Hong, Mingchen Zhuge, Jonathan Chen, Xiawu Zheng, Yuheng Cheng, Jinlin Wang, Ceyao Zhang, Zili
 542 Wang, Steven Ka Shing Yau, Zijuan Lin, et al. Metagpt: Meta programming for a multi-agent collaborative
 543 framework. In *The Twelfth International Conference on Learning Representations*, 2023.

544

545 Wenyi Hong, Wenmeng Yu, Xiaotao Gu, Guo Wang, Guobing Gan, Haomiao Tang, Jiale Cheng, Ji Qi,
 546 Junhui Ji, Lihang Pan, et al. Glm-4.1 v-thinking: Towards versatile multimodal reasoning with scalable
 547 reinforcement learning. *arXiv preprint arXiv:2507.01006*, 2025.

548

549 Wenxuan Huang, Bohan Jia, Zijie Zhai, Shaosheng Cao, Zheyu Ye, Fei Zhao, Yao Hu, and Shaohui Lin.
 550 Vision-r1: Incentivizing reasoning capability in multimodal large language models. *arXiv preprint*
 551 *arXiv:2503.06749*, 2025.

552

553 Xu Huang, Weiwen Liu, Xiaolong Chen, Xingmei Wang, Hao Wang, Defu Lian, Yasheng Wang, Ruiming
 554 Tang, and Enhong Chen. Understanding the planning of llm agents: A survey. *arXiv preprint*
 555 *arXiv:2402.02716*, 2024.

556

557 Aaron Jaech, Adam Kalai, Adam Lerer, Adam Richardson, Ahmed El-Kishky, Aiden Low, Alec Helyar, Aleksander
 558 Madry, Alex Beutel, Alex Carney, et al. Openai o1 system card. *arXiv preprint arXiv:2412.16720*,
 559 2024.

560

561 Yifan Jiang, Kexuan Sun, Zhivar Sourati, Kian Ahrabian, Kaixin Ma, Filip Ilievski, Jay Pujara, et al. Marvel:
 562 Multidimensional abstraction and reasoning through visual evaluation and learning. *Advances in Neural*
 563 *Information Processing Systems*, 37:46567–46592, 2024.

564

565 Justin Johnson, Bharath Hariharan, Laurens Van Der Maaten, Li Fei-Fei, C Lawrence Zitnick, and Ross
 566 Girshick. Clevr: A diagnostic dataset for compositional language and elementary visual reasoning. In
 567 *Proceedings of the IEEE conference on computer vision and pattern recognition*, pp. 2901–2910, 2017.

564 Alexander Kirillov, Eric Mintun, Nikhila Ravi, Hanzi Mao, Chloe Rolland, Laura Gustafson, Tete Xiao,
 565 Spencer Whitehead, Alexander C Berg, Wan-Yen Lo, et al. Segment anything. In *Proceedings of the*
 566 *IEEE/CVF international conference on computer vision*, pp. 4015–4026, 2023.

567

568 Ranjay Krishna, Yuke Zhu, Oliver Groth, Justin Johnson, Kenji Hata, Joshua Kravitz, Stephanie Chen, Yannis
 569 Kalantidis, Li-Jia Li, David A Shamma, et al. Visual genome: Connecting language and vision using
 570 crowdsourced dense image annotations. *International journal of computer vision*, 123:32–73, 2017.

571

572 Alina Kuznetsova, Hassan Rom, Neil Alldrin, Jasper Uijlings, Ivan Krasin, Jordi Pont-Tuset, Shahab Kamali,
 573 Stefan Popov, Matteo Mallochi, Alexander Kolesnikov, et al. The open images dataset v4: Unified image
 574 classification, object detection, and visual relationship detection at scale. *International journal of computer*
 575 *vision*, 128(7):1956–1981, 2020.

576

577 Lin Li, Guikun Chen, Hanrong Shi, Jun Xiao, and Long Chen. A survey on multimodal benchmarks: In the
 578 era of large ai models. *arXiv preprint arXiv:2409.18142*, 2024a.

579

580 Manling Li, Shiyu Zhao, Qineng Wang, Kangrui Wang, Yu Zhou, Sanjana Srivastava, Cem Gokmen, Tony
 581 Lee, Erran Li Li, Ruohan Zhang, et al. Embodied agent interface: Benchmarking llms for embodied
 582 decision making. *Advances in Neural Information Processing Systems*, 37:100428–100534, 2024b.

583

584 Zhuowan Li, Xingrui Wang, Elias Stengel-Eskin, Adam Kortylewski, Wufei Ma, Benjamin Van Durme, and
 585 Alan L Yuille. Super-clevr: A virtual benchmark to diagnose domain robustness in visual reasoning. In
 586 *Proceedings of the IEEE/CVF conference on computer vision and pattern recognition*, pp. 14963–14973,
 587 2023.

588

589 Tsung-Yi Lin, Michael Maire, Serge Belongie, James Hays, Pietro Perona, Deva Ramanan, Piotr Dollár, and
 590 C Lawrence Zitnick. Microsoft coco: Common objects in context. In *Computer vision–ECCV 2014: 13th*
 591 *European conference, zurich, Switzerland, September 6–12, 2014, proceedings, part v 13*, pp. 740–755.
 592 Springer, 2014.

593

594 Chen Cecilia Liu, Fajri Koto, Timothy Baldwin, and Iryna Gurevych. Are multilingual llms culturally-diverse
 595 reasoners? an investigation into multicultural proverbs and sayings. *arXiv preprint arXiv:2309.08591*,
 596 2023a.

597

598 Fan Liu, Wenshuo Chao, Naiqiang Tan, and Hao Liu. Bag of tricks for inference-time computation of llm
 599 reasoning. *arXiv preprint arXiv:2502.07191*, 2025a.

600

601 Fangyu Liu, Guy Emerson, and Nigel Collier. Visual spatial reasoning. *Transactions of the Association for*
 602 *Computational Linguistics*, 11:635–651, 2023b.

603

604 Junzhuo Liu, Xuzheng Yang, Weiwei Li, and Peng Wang. Finecops-ref: A new dataset and task for fine-
 605 grained compositional referring expression comprehension. *arXiv preprint arXiv:2409.14750*, 2024a.

606

607 Shilong Liu, Zhaoyang Zeng, Tianhe Ren, Feng Li, Hao Zhang, et al. Grounding dino: Marrying dino with
 608 grounded pre-training for open-set object detection. In *European Conference on Computer Vision*, pp.
 609 38–55. Springer, 2024b.

610

611 Weiwen Liu, Xu Huang, Xingshan Zeng, xinlong hao, Shuai Yu, Dexun Li, Shuai Wang, Weinan Gan,
 612 Zhengying Liu, Yuanqing Yu, Zezhong WANG, Yuxian Wang, Wu Ning, Yutai Hou, Bin Wang, Chuhan
 613 Wu, Wang Xinzhi, Yong Liu, Yasheng Wang, Duyu Tang, Dandan Tu, Lifeng Shang, Xin Jiang, Ruiming
 614 Tang, Defu Lian, Qun Liu, and Enhong Chen. ToolACE: Winning the points of LLM function calling.
 615 In *The Thirteenth International Conference on Learning Representations*, 2025b. URL <https://openreview.net/forum?id=8EB8k6DdCU>.

611 Yuan Liu, Haodong Duan, Yuanhan Zhang, Bo Li, Songyang Zhang, Wangbo Zhao, Yike Yuan, Jiaqi Wang,
 612 Conghui He, Ziwei Liu, et al. Mmbench: Is your multi-modal model an all-around player? In *European*
 613 *conference on computer vision*, pp. 216–233. Springer, 2024c.

614

615 Yuliang Liu, Zhang Li, Mingxin Huang, Biao Yang, Wenwen Yu, Chunyuan Li, Xu-Cheng Yin, Cheng-Lin
 616 Liu, Lianwen Jin, and Xiang Bai. Ocrbench: on the hidden mystery of ocr in large multimodal models.
 617 *Science China Information Sciences*, 67(12):220102, 2024d.

618

619 Ziyu Liu, Zeyi Sun, Yuhang Zang, Xiaoyi Dong, Yuhang Cao, Haodong Duan, Dahua Lin, and Jiaqi Wang.
 620 Visual-rft: Visual reinforcement fine-tuning. *arXiv preprint arXiv:2503.01785*, 2025c.

621

622 Chuofan Ma, Yi Jiang, Jiannan Wu, Zehuan Yuan, and Xiaojuan Qi. Groma: Localized visual tokenization for
 623 grounding multimodal large language models. In *European Conference on Computer Vision*, pp. 417–435.
 624 Springer, 2024.

625

626 Aman Madaan, Niket Tandon, Prakhar Gupta, Skyler Hallinan, Luyu Gao, Sarah Wiegreffe, Uri Alon, Nouha
 627 Dziri, Shrimai Prabhumoye, Yiming Yang, et al. Self-refine: Iterative refinement with self-feedback.
 628 *Advances in Neural Information Processing Systems*, 36:46534–46594, 2023.

629

630 Wujian Peng, Sicheng Xie, Zuyao You, Shiyi Lan, and Zuxuan Wu. Synthesize diagnose and optimize:
 631 Towards fine-grained vision-language understanding. In *Proceedings of the IEEE/CVF Conference on*
 632 *Computer Vision and Pattern Recognition*, pp. 13279–13288, 2024.

633

634 Bryan A Plummer, Liwei Wang, Chris M Cervantes, Juan C Caicedo, Julia Hockenmaier, and Svetlana
 635 Lazebnik. Flickr30k entities: Collecting region-to-phrase correspondences for richer image-to-sentence
 636 models. In *Proceedings of the IEEE international conference on computer vision*, pp. 2641–2649, 2015.

637

638 Pavan Kartheek Rachabatuni, Filippo Principi, Paolo Mazzanti, and Marco Bertini. Context-aware chatbot
 639 using mllms for cultural heritage. In *Proceedings of the 15th ACM Multimedia Systems Conference*, pp.
 640 459–463, 2024.

641

642 Olga Russakovsky, Jia Deng, Hao Su, Jonathan Krause, Sanjeev Satheesh, Sean Ma, Zhiheng Huang, Andrej
 643 Karpathy, Aditya Khosla, Michael Bernstein, et al. Imagenet large scale visual recognition challenge.
 644 *International journal of computer vision*, 115:211–252, 2015.

645

646 Gabriel Sarch, Lawrence Jang, Michael Tarr, William W Cohen, Kenneth Marino, and Katerina Fragkiadaki.
 647 Vlm agents generate their own memories: Distilling experience into embodied programs of thought.
 648 *Advances in Neural Information Processing Systems*, 37:75942–75985, 2024.

649

650 Christoph Schuhmann, Romain Beaumont, Richard Vencu, Cade Gordon, Ross Wightman, Mehdi Cherti,
 651 Theo Coombes, Aarush Katta, Clayton Mullis, Mitchell Wortsman, et al. Laion-5b: An open large-scale
 652 dataset for training next generation image-text models. *Advances in neural information processing systems*,
 653 35:25278–25294, 2022.

654

655 Hao Shao, Shengju Qian, Han Xiao, Guanglu Song, Zhuofan Zong, Letian Wang, Yu Liu, and Hongsheng Li.
 656 Visual cot: Advancing multi-modal language models with a comprehensive dataset and benchmark for
 657 chain-of-thought reasoning. *Advances in Neural Information Processing Systems*, 37:8612–8642, 2024.

658

659 Haozhan Shen, Peng Liu, Jingcheng Li, Chunxin Fang, Yibo Ma, Jiajia Liao, Qiaoli Shen, Zilun Zhang,
 660 Kangjia Zhao, Qianqian Zhang, et al. Vlm-r1: A stable and generalizable r1-style large vision-language
 661 model. *arXiv preprint arXiv:2504.07615*, 2025a.

658 Haozhan Shen, Kangjia Zhao, Tiancheng Zhao, Ruochen Xu, Zilun Zhang, Mingwei Zhu, and Jianwei
 659 Yin. Zoomeye: Enhancing multimodal llms with human-like zooming capabilities through tree-based
 660 image exploration. In *Proceedings of the 2025 Conference on Empirical Methods in Natural Language
 661 Processing*, pp. 6613–6629, 2025b.

662 Charlie Snell, Jaehoon Lee, Kelvin Xu, and Aviral Kumar. Scaling llm test-time compute optimally can be
 663 more effective than scaling model parameters. *arXiv preprint arXiv:2408.03314*, 2024.

665 Gemini Team, Petko Georgiev, Ving Ian Lei, Ryan Burnell, Libin Bai, Anmol Gulati, Garrett Tanzer, Damien
 666 Vincent, Zhufeng Pan, Shibo Wang, et al. Gemini 1.5: Unlocking multimodal understanding across millions
 667 of tokens of context. *arXiv preprint arXiv:2403.05530*, 2024.

668 Gemma Team, Aishwarya Kamath, Johan Ferret, Shreya Pathak, Nino Vieillard, Ramona Merhej, Sarah
 669 Perrin, Tatiana Matejovicova, Alexandre Ramé, Morgane Rivière, et al. Gemma 3 technical report. *arXiv
 670 preprint arXiv:2503.19786*, 2025a.

672 Kimi Team, Angang Du, Bohong Yin, Bowei Xing, Bowen Qu, Bowen Wang, Cheng Chen, Chenlin Zhang,
 673 Chenzhuang Du, Chu Wei, et al. Kimi-vl technical report. *arXiv preprint arXiv:2504.07491*, 2025b.

674 Yunjie Tian, Tianren Ma, Lingxi Xie, and Qixiang Ye. Chatterbox: Multimodal referring and grounding
 675 with chain-of-questions. *Proceedings of the AAAI Conference on Artificial Intelligence*, 39(7):7401–7409,
 676 Apr. 2025. doi: 10.1609/aaai.v39i7.32796. URL <https://ojs.aaai.org/index.php/AAAI/article/view/32796>.

678 Shengbang Tong, Zhuang Liu, Yuexiang Zhai, Yi Ma, Yann LeCun, and Saining Xie. Eyes wide shut?
 679 exploring the visual shortcomings of multimodal llms. In *Proceedings of the IEEE/CVF Conference on
 680 Computer Vision and Pattern Recognition*, pp. 9568–9578, 2024.

682 Peiyi Wang, Lei Li, Liang Chen, Zefan Cai, Dawei Zhu, Binghuai Lin, Yunbo Cao, Qi Liu, Tianyu Liu, and
 683 Zhifang Sui. Large language models are not fair evaluators. *arXiv preprint arXiv:2305.17926*, 2023.

685 Renxi Wang, Xudong Han, Lei Ji, Shu Wang, Timothy Baldwin, and Haonan Li. Toolgen: Unified tool retrieval
 686 and calling via generation. In *The Thirteenth International Conference on Learning Representations*, 2025.
 687 URL <https://openreview.net/forum?id=XLMAMmowdY>.

688 Weiyun Wang, Yiming Ren, Haowen Luo, Tiantong Li, Chenxiang Yan, Zhe Chen, Wenhui Wang, Qingyun
 689 Li, Lewei Lu, Xizhou Zhu, et al. The all-seeing project v2: Towards general relation comprehension of the
 690 open world. In *European Conference on Computer Vision*, pp. 471–490. Springer, 2024a.

692 Zhecan Wang, Garrett Bingham, Adams Wei Yu, Quoc V Le, Thang Luong, and Golnaz Ghiasi. Haloquest:
 693 A visual hallucination dataset for advancing multimodal reasoning. In *European Conference on Computer
 694 Vision*, pp. 288–304. Springer, 2024b.

695 Fangyun Wei, Jinjing Zhao, Kun Yan, Hongyang Zhang, and Chang Xu. A large-scale human-centric
 696 benchmark for referring expression comprehension in the lmm era. *Advances in Neural Information
 697 Processing Systems*, 37:69566–69587, 2024.

698 Jason Wei, Xuezhi Wang, Dale Schuurmans, Maarten Bosma, Fei Xia, Ed Chi, Quoc V Le, Denny Zhou, et al.
 699 Chain-of-thought prompting elicits reasoning in large language models. *Advances in neural information
 700 processing systems*, 35:24824–24837, 2022.

702 Penghao Wu and Saining Xie. V?: Guided visual search as a core mechanism in multimodal llms. In
 703 *Proceedings of the IEEE/CVF Conference on Computer Vision and Pattern Recognition*, pp. 13084–13094,
 704 2024.

705 Zhiyu Wu, Xiaokang Chen, Zizheng Pan, Xingchao Liu, Wen Liu, Damai Dai, Huazuo Gao, Yiyang Ma,
 706 Chengyue Wu, Bingxuan Wang, et al. Deepseek-vl2: Mixture-of-experts vision-language models for
 707 advanced multimodal understanding. *arXiv preprint arXiv:2412.10302*, 2024.

708 Linhui Xiao, Xiaoshan Yang, Fang Peng, Ming Yan, Yaowei Wang, and Changsheng Xu. Clip-vg: Self-paced
 709 curriculum adapting of clip for visual grounding. *IEEE Transactions on Multimedia*, 26:4334–4347, 2023.

710 Linhui Xiao, Xiaoshan Yang, Xiangyuan Lan, Yaowei Wang, and Changsheng Xu. Towards visual grounding:
 711 A survey. *arXiv preprint arXiv:2412.20206*, 2024.

712 Yunqiu Xu, Linchao Zhu, and Yi Yang. Mc-bench: A benchmark for multi-context visual grounding in the
 713 era of mllms. *arXiv preprint arXiv:2410.12332*, 2024.

714 Li Yang, Yan Xu, Chunfeng Yuan, Wei Liu, Bing Li, and Weiming Hu. Improving visual grounding with
 715 visual-linguistic verification and iterative reasoning. In *Proceedings of the IEEE/CVF Conference on*
 716 *Computer Vision and Pattern Recognition*, pp. 9499–9508, 2022.

717 Ruilin Yao, Shengwu Xiong, Yichen Zhao, and Yi Rong. Visual grounding with multi-modal conditional
 718 adaptation. In *Proceedings of the 32nd ACM International Conference on Multimedia*, pp. 3877–3886,
 719 2024.

720 Haoxuan You, Haotian Zhang, Zhe Gan, Xianzhi Du, Bowen Zhang, Zirui Wang, Liangliang Cao, Shih-Fu
 721 Chang, and Yinfei Yang. Ferret: Refer and ground anything anywhere at any granularity. *arXiv preprint*
 722 *arXiv:2310.07704*, 2023.

723 Haoxuan You, Haotian Zhang, Zhe Gan, Xianzhi Du, Bowen Zhang, Zirui Wang, Liangliang Cao, Shih-Fu
 724 Chang, and Yinfei Yang. Ferret: Refer and ground anything anywhere at any granularity. In *The Twelfth*
 725 *International Conference on Learning Representations*, 2024. URL <https://openreview.net/forum?id=2msbbX3yD>.

726 Peter Young, Alice Lai, Micah Hodosh, and Julia Hockenmaier. From image descriptions to visual denotations:
 727 New similarity metrics for semantic inference over event descriptions. *Transactions of the association for*
 728 *computational linguistics*, 2:67–78, 2014.

729 Licheng Yu, Patrick Poirson, Shan Yang, Alexander C Berg, and Tamara L Berg. Modeling context in
 730 referring expressions. In *European Conference on Computer Vision*, pp. 69–85. Springer, 2016.

731 Siyu Yuan, Kaitao Song, Jiangjie Chen, Xu Tan, Yongliang Shen, Kan Ren, Dongsheng Li, and Deqing
 732 Yang. Easytool: Enhancing llm-based agents with concise tool instruction. In *Proceedings of the 2025*
 733 *Conference of the Nations of the Americas Chapter of the Association for Computational Linguistics: Human Language Technologies (Volume 1: Long Papers)*, pp. 951–972, 2025.

734 Xiang Yue, Yuansheng Ni, Kai Zhang, Tianyu Zheng, Ruoqi Liu, Ge Zhang, Samuel Stevens, Dongfu Jiang,
 735 Weiming Ren, Yuxuan Sun, et al. Mmmu: A massive multi-discipline multimodal understanding and
 736 reasoning benchmark for expert agi. In *Proceedings of the IEEE/CVF Conference on Computer Vision and*
 737 *Pattern Recognition*, pp. 9556–9567, 2024.

738 Yuhang Zang, Wei Li, Jun Han, Kaiyang Zhou, and Chen Change Loy. Contextual object detection with
 739 multimodal large language models. *International Journal of Computer Vision*, 133(2):825–843, 2025.

740 Jiarui Zhang, Mahyar Khayatkhoei, Prateek Chhikara, and Filip Ilievski. Mllms know where to look:
 741 Training-free perception of small visual details with multimodal llms. *arXiv preprint arXiv:2502.17422*,
 742 2025a.

752 Wanyue Zhang, Yibin Huang, Yangbin Xu, JingJing Huang, Helu Zhi, Shuo Ren, Wang Xu, and Jiajun Zhang.
753 Why do mllms struggle with spatial understanding? a systematic analysis from data to architecture. *arXiv*
754 *preprint arXiv:2509.02359*, 2025b.

755 Yikai Zhang, Siyu Yuan, Caiyu Hu, Kyle Richardson, Yanghua Xiao, and Jiangjie Chen. Timearena: Shaping
756 efficient multitasking language agents in a time-aware simulation. In *Proceedings of the 62nd Annual*
757 *Meeting of the Association for Computational Linguistics (Volume 1: Long Papers)*, pp. 3894–3916, 2024a.

758 Zeyu Zhang, Quanyu Dai, Xiaohe Bo, Chen Ma, Rui Li, Xu Chen, Jieming Zhu, Zhenhua Dong, and Ji-Rong
759 Wen. A survey on the memory mechanism of large language model-based agents. *ACM Transactions on*
760 *Information Systems*, 43(6):1–47, 2025c.

761 Zhehao Zhang, Ryan Rossi, Tong Yu, Franck Dernoncourt, Ruiyi Zhang, Jiuxiang Gu, Sungchul Kim, Xiang
762 Chen, Zichao Wang, and Nedim Lipka. Vipact: Visual-perception enhancement via specialized vlm agent
763 collaboration and tool-use. *arXiv preprint arXiv:2410.16400*, 2024b.

764 Zicheng Zhang, Haoning Wu, Erli Zhang, Guangtao Zhai, and Weisi Lin. Q-bench: A benchmark for
765 multi-modal foundation models on low-level vision from single images to pairs. *IEEE Transactions on*
766 *Pattern Analysis and Machine Intelligence*, 2024c.

767 Chuyang Zhao, YuXin Song, Junru Chen, Kang Rong, Haocheng Feng, Gang Zhang, Shufan Ji, Jingdong
768 Wang, Errui Ding, and Yifan Sun. Octopus: A multi-modal llm with parallel recognition and sequential
769 understanding. *Advances in Neural Information Processing Systems*, 37:90009–90029, 2024.

770 Jinguo Zhu, Weiyun Wang, Zhe Chen, Zhaoyang Liu, Shenglong Ye, Lixin Gu, Yuchen Duan, Hao Tian,
771 Weijie Su, Jie Shao, et al. Internvl3: Exploring advanced training and test-time recipes for open-source
772 multimodal models. *arXiv preprint arXiv:2504.10479*, 2025.

773 Zhuofan Zong, Bingqi Ma, Dazhong Shen, Guanglu Song, Hao Shao, Dongzhi Jiang, Hongsheng Li, and
774 Yu Liu. Mova: Adapting mixture of vision experts to multimodal context. *Advances in Neural Information*
775 *Processing Systems*, 37:103305–103333, 2024.

776

777

778

779

780

781

782

783

784

785

786

787

788

789

790

791

792

793

794

795

796

797

798

799 **A APPENDIX**
800801 **A.1 RELATED WORK**
802803 **A.1.1 BENCHMARKS FOR VISUAL CAPABILITY OF MLLMs**
804

805 The capability of Visual Perception, Understanding and Reasoning is a foundational aspect of understanding
 806 benchmarks, which involves the ability to recognize and localize multiple objects, interpret various visual
 807 elements with complex emotional or implicit cues and summarize visual information for feedback and
 808 decision making (Li et al., 2024b). Specifically, Perception in MLLMs involves the classification, detection of
 809 basic visual objects (*e.g.*, dog, cat) and attributes (*e.g.*, color, lighting). These low-level perceptual capabilities
 810 are crucial for various applications, including recognition systems (Zhao et al., 2024) and visual quality
 811 enhancement (Zhang et al., 2024c). Understanding represents a sophisticated level of image understanding
 812 that focuses on the detailed and nuanced aspects of visual content. It includes recognizing and interpreting
 813 the visual-linguistic concepts, such as text recognition (OCRBench (Liu et al., 2024d)), Visual Grounding
 814 (RefCOCO (Yu et al., 2016), FineCops-Ref (Liu et al., 2024a), HC-RefLoCo (Wei et al., 2024)) and Referring
 815 Expression Generation (Visual Genome) (Krishna et al., 2017), which refers to the model’s ability to accurately
 816 link visual elements with corresponding textual descriptions. Although tasks at this level begin to involve
 817 visual and textual alignment, they still do not require reasoning or external knowledge. For higher-order
 818 capability, reasoning in MLLMs involves advanced event understanding and deep meaning extraction from
 819 multimodal data. These capabilities include interpreting and responding to complex emotional cues across
 820 multiple modalities (Cheng et al., 2024), deriving subtle implicit meanings from visual and contextual
 821 information (Liu et al., 2023a), and a range of other competencies, including knowledge acquisition, language
 822 generation, spatial awareness, and cultural context integration (Rachabatuni et al., 2024).

823 **A.1.2 REASONING CAPABILITY OF MLLMs**
824

825 MLLMs have demonstrated remarkable reasoning capabilities, largely facilitated by test-time scaling (Dong
 826 et al., 2022; Wei et al., 2022), which allows feeding prompted samples and context. This capability has been
 827 further enhanced by chain-of-thought (CoT) prompting (Wei et al., 2022), which enables LLMs to generate
 828 coherent intermediate reasoning steps toward the final answer. Previous studies have shown that LLMs benefit
 829 from manually written demonstrations as well as zero-shot prompting outputs. However, due to the domain
 830 gap between various modalities, the current reasoning capability of MLLMs in the complex real-world
 831 environment is still limited. To address this limitation, researchers have focused on enhancing the reasoning
 832 capability of MLLMs in both the training and prompting paradigms. Flamingo (Alayrac et al., 2022) bridges
 833 the gap between these two modalities by pre-training on interleaved visual and textual data. Some other
 834 works, such as Shikra (Chen et al., 2023b) and Ferret (You et al., 2023), leverage visual grounding data (Xiao
 835 et al., 2024; Yao et al., 2024) to achieve fine-grained vision-language alignment. Furthermore, recent studies
 836 have also demonstrated that augmenting computing resources during the testing phase (test-time scaling) can
 837 enhance the reasoning capabilities of LLMs (Jaech et al., 2024). More specifically, Prompt-based Reasoning
 838 Meta-Systems (PRMS) can be employed to guide LLMs in evaluating and filtering intermediate “thinking”
 839 processes (Snell et al., 2024). This encourages the generation of more sophisticated reasoning steps during
 840 testing, ultimately leading to improved reasoning accuracy. Beyond that, some methods employ the external
 841 knowledge to focus on important visual details, like V* (Wu & Xie, 2024), Marvel (Jiang et al., 2024), and
 842 ICAL (Sarch et al., 2024), collecting a series of visual reasoning steps as training data. More recently, with
 843 the emergence of DeepSeek-R1 (Guo et al., 2025) demonstrating strong potential in LLM reasoning, research
 844 efforts have begun to explore reasoning-centric models and R1-style reinforcement learning strategies for
 845 understanding complex visual scenes and tasks. These studies (Huang et al., 2025; Shen et al., 2025a; Liu
 846 et al., 2025c) particularly emphasize the long-chain reasoning capabilities within MLLMs, aiming to enhance
 847 their performance in handling intricate visual-linguistic reasoning challenges.

846
847

A.1.3 LLM-BASED AGENTIC REASONING

848
849
850
851
852
853
854
855
856
857
858
859
860
861
862
863
864
865

The rapid progress of large language models (Achiam et al., 2023; Bai et al., 2025) has sparked significant interest in building autonomous agents capable of solving complex, multi-step reasoning tasks. Leveraging the strong chain-of-thought (CoT) abilities of modern LLMs (Wei et al., 2022), these systems typically decompose a complex problem into a sequence of structured subtasks, invoke intermediate deliberation, and integrate the resulting insights to produce a final answer (Gupta & Kembhavi, 2023; Chen et al., 2023a). Recent developments in LLM-based autonomous agents highlight the importance of planning (Huang et al., 2024; Zhang et al., 2024a), tool usage (Yuan et al., 2025), memory (Zhang et al., 2025c), and persona (Chen et al., 2024a). In parallel, multi-agent frameworks such as MetaGPT (Hong et al., 2023), AgentVerse (Chen et al., 2023c), etc., demonstrate strong performance by orchestrating multiple interacting agents, often instantiated as distinct roles with specialized responsibilities. Despite their success, these systems rely heavily on manually designed personas, fixed role hierarchies, or hand-crafted coordination rules, which limits their flexibility and generalization across tasks and domains. Moreover, the dependence on external scaffolding or pre-specified agent behaviors often restricts the model’s ability to adaptively adjust its internal reasoning pathway. To address these limitations, SMEC introduces a self-driven agentic reasoning mechanism that automatically generates diverse experts, elicits their reasoning, filters redundant experts, and synthesizes their perspectives into a final consensus, all within the model’s own language-native inference loop.

866
867
868

A.2 SPECIFIC DEFINATION OF DIFFERENT TASKS

869
870
871

Object Counting (OC): Estimating the number of object instances described by a free-form expression, often under complex conditions like occlusion, scale variation, or clutter.

872
873

Object Detection (OD): Localizing objects within an image by generating bounding boxes paired with corresponding class labels. In order to better match the real-life scenarios and practical applications, we construct more than 500 fine-grained object categories based on natural language.

874
875
876

Object Existence Determination (OE): Determining whether a particular object, which described by a detailed expression, exists in the image without requiring spatial localization.

877
878
879

Relation Extraction (RE): Identifying semantic relationships (e.g., “holding”, “next to”, “wearing”) between pairs of objects to facilitate structured scene understanding. And we added questions about the objects that do not exist in the images to evaluate model’s ability to suppress hallucinations.

880
881

Visual Grounding (VG): Localizing an image region that corresponds to a natural language expression, linking linguistic references to fine-grained visual content.

882
883
884
885
886

Region-wise OCR (OCR): Recognizing and transcribing text within a region, which specified by coordinates or description, facilitating fine-grained interleaved image-text understanding.

887
888
889
890
891
892

Spatial Relationship Comprehension (SRC): Understanding geometric relationships (e.g., “above” and “to the left front to”) between objects within diverse 3D views, supporting visual-spatial reasoning. Compared to some rudimentary or synthetic spatial understanding datasets (Johnson et al., 2017; Li et al., 2023; Liu et al., 2023b), our data is more realistic in emphasizing spatial location understanding under real-world scenarios as well as 2D images acquired by cameras or cell phones.



Figure 7: Lens covers a wide range of images and annotations, from fine-grained recognition and spatial localization to complex reasoning over extended thought processes. Notably, each image is annotated with labels corresponding to all subtasks concurrently, enabling comprehensive evaluation.

940
941

A.3 QUALITY CONTROL PROCESS

942
943
944
945

In addition to the annotations, diversified measures were taken to enrich the content of data samples and ensure their quality. Specifically, we implemented a multi-faceted quality control process. Beyond a two-step data cleaning protocol, we also enriched each image with supplementary metadata to facilitate traceability and contextual analysis.

946
947
948
949

First, we manually performed a two-stage data cleaning process. In the initial stage, we reviewed and eliminated suspected duplicate images. The second stage involved distributing the problems among co-authors for meticulous format and typo checking, ensuring all annotations adhered to a standardized format.

950
951
952
953
954
955

To further validate the quality and consistency of our annotations, we performed an additional two-step verification process. This included both manual and machine-assisted checks. The entire dataset was cross-verified by both an independent team of annotators and the Qwen2.5-VL 72B open-source model. For machine validation, we input the original image, question, and answer into the MLLM. Cases flagged as invalid by the model were isolated for manual re-evaluation by a separate team of annotators. For object detection and visual grounding tasks, we directly visualized the annotations on the images, enabling human evaluators to assess the validity of the bounding boxes.

956
957
958
959
960
961

Additionally, we enriched each image with supplementary metadata. We included a pseudonymized Annotator ID to allow for annotator-specific quality tracking while preserving privacy. The Time of Online Publication and Scene Category were also labeled to facilitate temporal studies, filter outdated content, and organize the dataset by scene. Finally, ambiguous images that consistently resulted in low inter-annotator agreement were manually filtered out to ensure a high-quality final dataset. Some cleaned representative examples are visualized in Figure 7.

962

A.4 DATA PRIVACY PROTECTION AND COPYRIGHT STATEMENT

963
964

Our protocol for handling potentially sensitive information was a multi-stage process designed to be as thorough as possible:

965
966
967
968
969
970

Automated Pre-screening: As an initial step, we used automated tools (*e.g.*, face detection models³, docTR⁴) to perform a preliminary scan of the collected images. This scan was configured to flag images with a high probability of containing human faces or dense blocks of text that might constitute personally identifiable information.

971
972
973
974
975
976

Comprehensive Manual Review: Every image, including those not flagged by the automated scan, was then subjected to a thorough manual review by our team of over 20 trained human annotators. Annotators received specific training and a detailed guide on identifying a wide range of sensitive data, including but not limited to: Visible and recognizable faces; Full names, usernames, or contact information; License plates, street addresses, or other specific location markers; Private documents or screens displaying personal data.

977
978

Sensitive Information Exclusion: Based on the manual review, if an image contained sensitive information, one of two actions was taken as mentioned in the paper:

979
980
981
982
983
984

- Processing: If the sensitive information was incidental to the image’s main content, we applied irreversible blurring or masking to the specific region.
- Exclusion: If the sensitive information was central to the image and could not be adequately anonymized without destroying the scene’s context, the image was entirely excluded from the final dataset.

985
986

³<https://github.com/timesler/facenet-pytorch>

⁴<https://github.com/mindee/doctr>

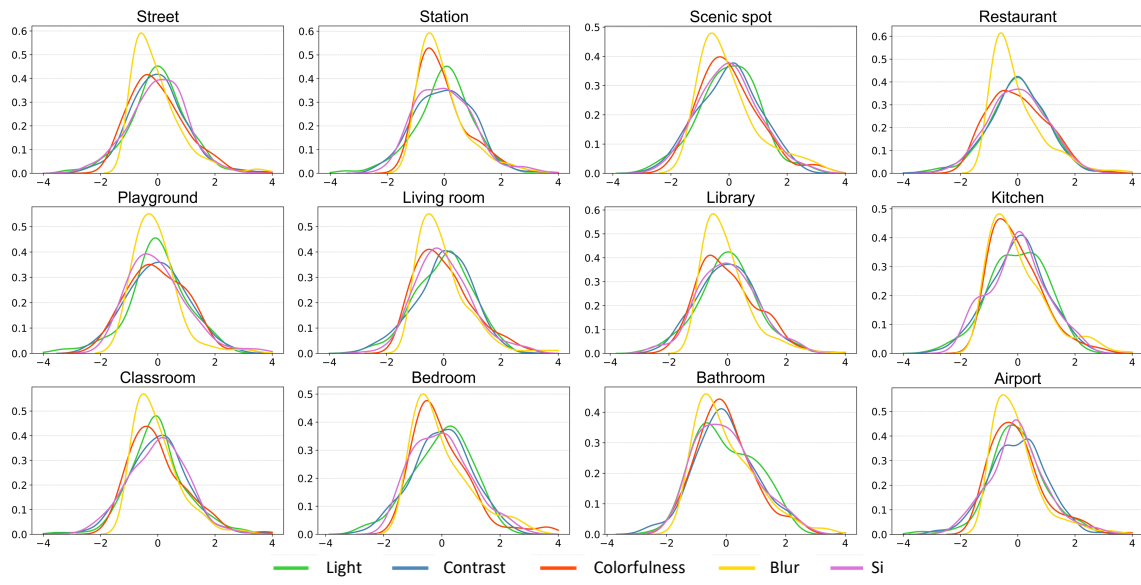


Figure 8: The normalized probability distributions of low-level attributes from different scenes. Scenes with flat peaks show more diversity, while those with sharp peaks have similar features.

Final Verification: To ensure consistency and quality, a final audit was conducted by a subset of the paper’s authors. This team reviewed a random sample of the approved images and 100% of the processed (blurred/masked) images to verify that our privacy protocol was correctly and consistently applied.

This multi-stage, human-centric approach ensures that the images in the `Lens` dataset comply with platform policies and respect individual privacy.

A.5 LOW-LEVEL FEATURE ANALYSIS OF IMAGES FROM DIFFERENT SCENES

We counted five low-level visual attributes, including lighting, contrast, color, blur, and spatial information (SI), to assess the statistical difference between different scenes. As shown in Figure 8, the normalized probability density curves of low-level visual attributes across different scenes are consistent with human perceptual preferences. Scenes with regulated lighting conditions (*e.g.*, classrooms, airports, and stations) demonstrate sharp peaks near $x \approx 0$ in the illumination curves (density > 0.5), indicating constrained variations in brightness. In contrast, domestic environments (*e.g.*, living rooms, bedrooms, and kitchens) display broader illumination distributions, suggesting more diverse and adaptive light sources. Furthermore, functional scenes such as bedrooms, bathrooms, and kitchens exhibit sharp, concentrated peaks in color distributions (peak density ≈ 0.5), implying greater structural regularity in specific visual attributes.

A.6 FINE-GRAINED EVALUATION OF VG

We conducted a fine-grained evaluation of a diverse set of models on the Visual Grounding (VG) task, categorizing them into two groups: traditional predictive multimodal models and generative multimodal large language models (MLLMs). The results, summarized in Table 4, reveal several key insights into the current state of visual grounding capabilities.

1034 A.6.1 COMPARISON OF MODEL CATEGORIES
1035

1036 The results clearly indicate a significant performance gap between the two model categories. The top-
1037 performing MLLMs, specifically Qwen2.5-VL-7B and Qwen2.5-VL-32B, demonstrate superior performance
1038 across all metrics, with an accuracy of 46.94% and 48.47% at $IoU@0.5$, respectively. This performance
1039 is substantially higher than the top predictive model, G-DINO, which achieves 37.05% at the same metric.
1040 This finding suggests that the generative and in-context learning capabilities of modern MLLMs provide
1041 a substantial advantage in the complex VG task, enabling them to better understand nuanced linguistic
1042 instructions and ground them accurately in the visual space.

1043 A.6.2 PERFORMANCE ON DIFFERENT SCALES
1044

1045 A multi-scale analysis, measured by accuracy on small (ACC_s), medium (ACC_m), and large (ACC_l) objects,
1046 provides a more granular view of each model’s strengths and weaknesses. Both traditional and generative
1047 models exhibit a similar trend: performance consistently improves with the size of the target object. This
1048 is a common challenge in visual grounding and object detection, as localizing and grounding small objects
1049 remains difficult.

1050 **Traditional Models:** Among the traditional models, G-DINO demonstrates a more balanced performance
1051 across scales, achieving 24.87% on small objects and 52.32% on large objects. In contrast, models like VLTVG
1052 and SimVG struggle significantly with small objects, with accuracies of 0.00% and 0.01% respectively, but
1053 show strong performance on large objects (29.70% and 45.20%).

1054 **Generative MLLMs:** While MLLMs also struggle with small objects, their performance is notably better
1055 than most traditional models. Qwen2.5-VL-32B and Qwen2.5-VL-7B achieve high accuracy on medium and
1056 large objects, with their ACC_m and ACC_l scores reaching 55.04% and 61.48% (for Qwen2.5-VL-32B), and
1057 54.12% and 60.24% (for Qwen2.5-VL-7B) respectively. The strong performance on larger objects may be
1058 attributed to their powerful visual backbones and advanced language understanding capabilities, which help
1059 them better contextualize the target within the scene.

1060 A.6.3 IMPACT OF MODEL ARCHITECTURE AND SIZE
1061

1062 Our results also highlight the importance of model architecture and size. The Qwen2.5-VL family of models,
1063 with its impressive performance, benefits from a powerful visual encoder (FE-ViT) and a sophisticated
1064 Qwen2.5 language backbone. Similarly, the InternVL3 series shows a clear scaling effect, where performance
1065 on most metrics improves as the model size increases from 2B to 14B. The performance of the 38B variant is
1066 slightly lower than the 14B variant due to its different visual backbone. This trend, consistent with findings in
1067 large language models, suggests that scaling up both visual and linguistic components is a promising direction
1068 for future research in visual grounding.

1069 A.7 MORE SYNERGISTIC EFFECTS ANALYSIS
1070

1071 We further notice that Figure 6 (a) shows OC-OCR correlation (0.77) \gg OC-OE (0.46). This contradicts
1072 intuition—object counting (OC) should align more naturally with existence checks (OE) than OCR. We
1073 attribute this to two factors. First, the Object Existence (OE) task is a simple binary classification: either an
1074 object is present or it is not. It requires a model to make a broad, scene-level assessment. In contrast, Object
1075 Counting (OC) is a more demanding task that requires fine-grained localization of individual objects, followed
1076 by an enumeration step. A model can be highly proficient at a binary existence check without possessing the
1077 precise localization and counting skills needed for the OC task. This fundamental difference in cognitive
1078 demand limits the correlation between the two. Second, the high correlation between Object Counting (OC)
1079 and OCR is not coincidental. Both tasks rely on a critical shared capability: fine-grained localization. To
1080 perform well on the OC task, a model must accurately identify and localize each instance of an object to

1081	1082	Method	Visual Backbone	Linguistic Backbone	Accuracy @ IoU					Scale-wise Accuracy		
					@0.5	@0.6	@0.7	@0.8	@0.9	ACC_s	ACC_m	ACC_l
1083 Methods based on predictive multimodal models:												
1084	TransVG (Deng et al., 2021)	RN101	BERT-B	8.73	7.57	6.29	4.40	1.69	0.01	2.01	23.64	
1085	VLTVG (Yang et al., 2022)	RN101	BERT-B	11.04	9.60	7.75	5.33	1.99	0.00	2.80	29.70	
1086	MMCA (Yao et al., 2024)	RN101	BERT-B	10.92	9.45	7.90	5.64	2.22	0.03	2.79	29.31	
1087	CLIP-VG (Xiao et al., 2023)	CLIP-B	CLIP-B	8.73	7.57	6.29	4.40	1.69	0.01	2.01	23.64	
1088	EEVG (Che et al., 2024c)	ViT-B/16	BERT-B	9.27	5.78	2.51	0.48	0.05	0.01	0.98	26.12	
1089	SimVG (Dai et al., 2024)	BEIT-3	BEIT-3	16.46	13.90	11.12	7.44	2.70	0.01	3.10	45.20	
	G-DINO (Liu et al., 2024b)	Swin-L	BERT-B	37.05	33.92	29.20	22.57	11.36	24.87	37.54	52.32	
1090 Methods based on generative multimodal large language models:												
1091	Groma-7B (Ma et al., 2024)	DINOv2-L	Vicuna	33.59	29.95	25.47	18.73	8.52	11.58	33.91	58.59	
1092	Mova-7B (Zong et al., 2024)	Multi-expert	Vicuna	20.44	13.10	5.98	1.09	0.13	5.06	15.97	40.36	
1093	Ferret-7B (You et al., 2024)	CLIP-L	Vicuna	23.26	18.97	13.95	7.61	1.84	1.85	19.49	54.64	
1094	Ferret-13B (You et al., 2024)	CLIP-L	Vicuna	24.20	19.81	14.41	8.12	2.05	2.26	20.42	56.31	
1095	InternVL3-2B (Zhu et al., 2025)	InternViT-0.3B	Qwen2.5	7.89	5.10	2.85	1.36	0.33	0.61	3.46	19.34	
1096	InternVL3-8B (Zhu et al., 2025)	InternViT-0.3B	Qwen2.5	17.54	13.23	8.89	4.94	1.60	3.23	15.36	35.21	
1097	InternVL3-14B (Zhu et al., 2025)	InternViT-0.3B	Qwen2.5	29.53	23.98	17.25	10.05	3.00	4.58	27.80	57.07	
1098	InternVL3-38B (Zhu et al., 2025)	InternViT-6B	Qwen2.5	27.85	21.42	15.00	8.23	2.37	4.91	25.81	53.56	
	VLM-R1-3B (Shen et al., 2025a)	FE-ViT	Qwen2.5	23.79	19.91	15.65	10.53	4.31	8.15	22.84	40.94	
	Qwen2.5-VL-3B (Bai et al., 2025)	FE-ViT	Qwen2.5	45.03	37.92	29.33	18.48	6.51	29.14	50.54	57.15	
	Qwen2.5-VL-7B (Bai et al., 2025)	FE-ViT	Qwen2.5	46.94	39.39	29.94	18.38	6.26	28.87	54.12	60.24	
	Qwen2.5-VL-32B (Bai et al., 2025)	FE-ViT	Qwen2.5	48.47	40.66	30.78	19.15	6.63	30.93	55.04	61.48	

Table 4: Multi-scale evaluation results.

count it. Similarly, to perform region-wise OCR, the model must first precisely locate the bounding box of the text before reading it. The strong correlation suggests that the ability to perform precise object localization is a dominant factor in a model’s success on both tasks, thus strengthening their relationship despite their different end goals.

To further test the synergy between different tasks, we conducted a experiment with Qwen2.5-VL-7B on a sampled subset of Lens. Specifically, when testing the SKI task, we fed the VQA question-answer pairs of other tasks into the model as context along with the question, and asked it to return the answer (refer to Appendix A.15 for the prompt template p_s , where we provide an example based on the OCR task). The test results are shown in Table 5 and reveal several noteworthy patterns. First, incorporating OCR information yields a substantial performance gain (from 39.80% to 41.36%), indicating that understanding scene text helps the model solve some reasoning tasks. Second, although some tasks—such as OE and OC—exhibit limited or even negative effects when introduced individually, their combination with OCR consistently boosts performance. This may indicate that auxiliary perceptual signals, while insufficient on their own, can enhance reasoning when mediated through textual understanding. Furthermore, the observed synergistic effects resonate with the design philosophy of our proposed Self-Driven Multi-Expert Collaborative (SMEC) framework. We argue that complex multimodal reasoning cannot be achieved by isolated competencies alone, but requires a structured mechanism to coordinate heterogeneous sources of evidence.

1119	OCR	-	✓	-	-	-	✓	✓	✓	✓	✓	✓
1120	RE	-	-	✓	-	-	✓	-	-	✓	✓	✓
1121	OE	-	-	-	✓	-	-	✓	-	✓	-	✓
1122	OC	-	-	-	-	✓	-	-	✓	-	✓	✓
1123	Performance	39.80	41.36	38.03	39.23	39.52	40.72	41.45	40.73	41.93	40.79	41.90

Table 5: Testing the synergistic effects of different tasks on Scene Knowledge Inference (SKI).

1128 A.8 ANALYSIS OF INPUT RESOLUTION
1129
1130

Method	Visual Backbone	Linguistic Backbone	Accuracy @ Input Resolution			
			640 × 640	960 × 960	1280 × 1280	1600 × 1600
InternVL3-2B (Zhu et al., 2025)	InternViT-0.3B	Qwen2.5	40.97	41.53	41.90	40.60
InternVL3-9B (Zhu et al., 2025)	InternViT-0.3B	InternLM3-8B	46.95	46.54	46.65	46.63
InternVL3-14B (Zhu et al., 2025)	InternViT-0.3B	Qwen2.5	50.28	51.15	51.58	51.17
InternVL3-38B (Zhu et al., 2025)	InternViT-6B	Qwen2.5	50.88	50.97	49.98	51.08
Qwen2.5-VL-3B (Bai et al., 2025)	FE-ViT	Qwen2.5	40.08	40.44	40.48	40.58
Qwen2.5-VL-7B (Bai et al., 2025)	FE-ViT	Qwen2.5	46.52	47.41	48.13	48.11
Qwen2.5-VL-32B (Bai et al., 2025)	FE-ViT	Qwen2.5	53.72	54.37	54.10	54.09
GLM-4.1V-Base-9B (Hong et al., 2025)	AlMv2-Huge	GLM-4-0414	42.35	42.86	43.28	43.73
GLM-4.1V-Thinking-9B (Hong et al., 2025)	AlMv2-Huge	GLM-4-0414	48.77	50.78	51.32	51.13

1139 Table 6: Benchmark results across varying input resolutions.
1140
1141

1142 We conducted a detailed analysis to understand the impact of varying input resolutions on model performance.
1143 The results, summarized in Table 6, reveal several key insights.

1144 **General Trend (Performance Improves with Resolution):** For most models, performance generally
1145 improves as the input resolution increases. This trend is evident in models such as Qwen2.5-VL-7B, which
1146 shows a steady increase in accuracy from 46.52% at 640×640 to 48.13% at 1280x1280. Similarly, GLM-4.1V-
1147 Thinking-9B improves from 48.77% to 51.32% over the same range. This is expected, as higher resolutions
1148 provide more visual detail, which is particularly beneficial for complex visual grounding and reasoning tasks
1149 that require fine-grained perception.

1150 **The Point of Diminishing Returns:** However, the results also suggest a point of diminishing returns. For
1151 many models, the performance gain from increasing the resolution beyond 1280x1280 is minimal, and in
1152 some cases, performance slightly decreases. For example, InternVL3-14B peaks at 51.58% at 1280x1280
1153 and then slightly drops to 51.17% at 1600x1600. Similarly, Qwen2.5-VL-7B’s performance plateaus at
1154 1280×1280. This phenomenon could be attributed to several factors, including the model’s architecture,
1155 which may not be fully optimized to handle the extra high-resolution information, or the fact that the added
1156 detail does not contribute meaningfully to solving the task.

1157 **Model-Specific Variations:** Interestingly, some models, like InternVL3-2B, show less sensitivity to resolution
1158 changes, with its performance remaining relatively stable across all resolutions. In contrast, models such as
1159 GLM-4.1V-Thinking-9B and Qwen2.5-VL-32B demonstrate a more pronounced performance improvement
1160 with higher resolutions, indicating that their architectures are more capable of leveraging the extra visual
1161 information. This suggests that the optimal input resolution is not a one-size-fits-all solution and depends
1162 heavily on the model’s architecture and design.

1163 A.9 QUALITATIVE ERROR ANALYSIS
1164

1165 To better illustrate common failure patterns and the underlying limitations of current Multimodal Large
1166 Language Models, we conduct a qualitative analysis of representative error cases across different task levels.
1167 Following the structure of our benchmark, we group the visualizations into two categories: (1) VQA-style
1168 tasks and (2) Localization tasks, including detection and visual grounding, as shown in Figure 9.

1169 For Perception & Understanding Tasks, they primarily require directly aligning visual content with textual
1170 queries. While modern MLLMs achieve reasonably high accuracy, their errors frequently stem from low-level
1171 perceptual limitations such as small objects, occlusion, distant subjects, and sensitivity to resolution. Several
1172 examples clearly illustrate this issue—for instance, miscounting the number of cyclists in a street scene, or
1173 failing to detect objects like a straw on a desk or a road light partially obscured by signage. For more complex
1174 reasoning tasks, we observe two major classes of systematic errors.

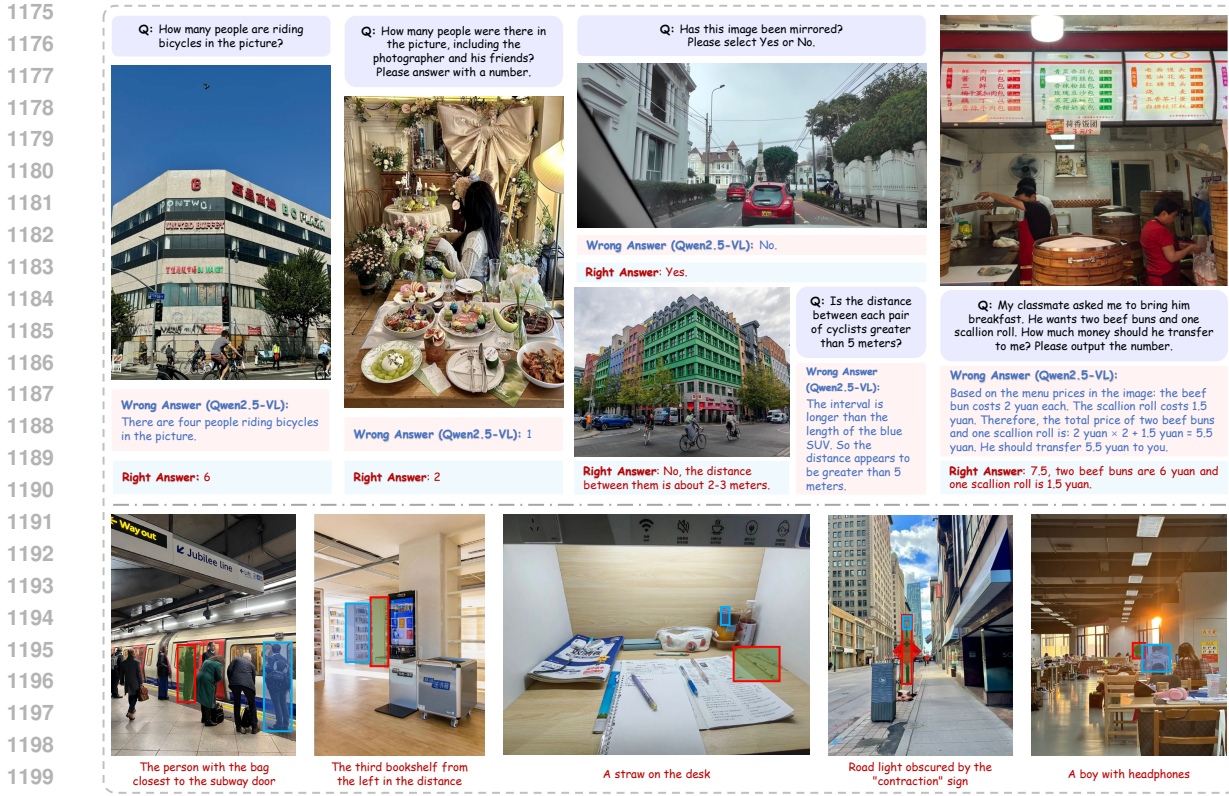


Figure 9: Failure cases for various tasks. Incorrect predictions and labels are indicated by blue and red, respectively

Correct reasoning, incorrect perception: The model often demonstrates sound logical reasoning but bases its inference on incorrect or incomplete visual extraction. For example, in a price-computation task, although the model performs the arithmetic correctly, it misreads the menu price of the beef bun, leading to a wrong total (5.5 instead of 7.5 yuan). This reveals a persistent bottleneck where high-level reasoning is constrained by low-level perception, especially OCR and fine-grained attribute recognition. Such cases motivate the need for agent-based or expert-collaborative pipelines—like our SMEC framework—which can iteratively refine visual cues or invoke specialized perception experts. They also highlight the importance of dynamic zoom-in strategies for capturing critical but small textual or visual details. (Wu & Xie, 2024; Zhang et al., 2025a; Shen et al., 2025b; Shao et al., 2024)

Spatial and physical reasoning deficits: A second recurring failure mode involves questions requiring geometric or physical commonsense. Models frequently struggle with tasks that implicitly require depth understanding, object-scale priors, or spatial metric reasoning. For instance, the model incorrectly concludes that two cyclists are more than 5 meters apart by comparing them to the length of a blue SUV, even though the correct distance is only about 2–3 meters. Likewise, it fails to judge whether an image is mirrored due to misunderstanding spatial layout cues. These issues echo recent findings showing that current MLLMs still lack robust spatial grounding, metric reasoning, and physical commonsense. (Zhang et al., 2025b; Azzolini et al., 2025)

1222 A.10 A FORMAL DESCRIPTION OF SMEC
1223

1224 As shown in Algorithm 1. A key advantage of SMEC is that it does not depend on fixed, hand-crafted prompts.
 1225 Instead, the prompts and expert descriptions are self-generated by the model based on the given visual input
 1226 and question. During each iteration, the model adaptively refines its expert descriptions and updates the
 1227 generation process when redundancy or low-quality information is detected. This adaptive design means
 1228 that SMEC is not tied to a specific phrasing or a predefined set of experts, but can flexibly adjust to different
 1229 problems and question types. As a result, our method is more robust than approaches that rely heavily on
 1230 manually designed prompts, since the “experts” in SMEC emerge dynamically from the model itself rather
 1231 than being externally imposed.

1232

1233

Algorithm 1 Self-driven Multi-Expert Generation & Collaboration

1234 **Initialization:** Based Instruction-tuned MLLM θ , Question q , Meta Generation Prompt
 1235 p_g , Inspection prompt p_i , Collaboration Prompt p_c , Description Set $D = \emptyset$, Maximum
 1236 Answer Set $A = \emptyset$, Iterations N_t .

```

1237 1:  $a_0 = \theta(q)$ ,  $A = A \cup a_0$                                 # Initial answer for question.
1238 2: for  $t = 1, 2, \dots, N_t$  do
1239 3:   if  $t = 1$  then
1240 4:      $d_q^1 = \theta(p_g, q, A_0)$                                 # Initial expert description.
1241 5:   else
1242 6:      $d_q^t = \theta(p_g, D, q, A_t)$       # New description based on existing information.
1243 7:   end if
1244 8:   if  $\theta(p_i, D, d_q^t) = \text{Retain}$  then
1245 9:      $D = D \cup d_q^t$                                 # Checking process.
1246 10:     $a_t = \theta(q, d_q^t)$ ,  $A = A \cup a_t$       # New answer from the expert perspective.
1247 11:   else
1248 12:      $p_g = \theta(q, d_q^t, p_g, D)$  # Update generation prompt while repeat descriptions.
1249 13:   end if
1250 14: end for
1251 15:  $a_{final} = \theta(q, A, p_c, D)$                                 # Summarize the final answer.

```

1252

1253

1254

A.11 HUMAN PREFERENCE

1255

1256 To ensure the verifiability of our evaluation, particularly for open-ended reasoning tasks, we employed a
 1257 large language model (LLM) as an automatic grader. To mitigate the concern regarding potential LLM
 1258 hallucinations or failure to detect nuanced mistakes, it is noted that the LLM grader (e.g., GLM4-flash) is
 1259 used to compare the model-generated responses against our pre-existing, human-annotated answers, ensuring
 1260 that the ground truth remains anchored in high-quality human data. We also conducted a human preference
 1261 analysis on a representative and complex task SKI with a subset of the dataset, aiming to provide a gold
 1262 standard against which to measure the reliability of judgement model. We recruited a separate team of ten
 1263 expert annotators who were not involved in the original data collection to manually evaluate the accuracy of
 1264 the model’s answers compared to the labeled answers, as shown in Table 7. In this setup, Actual Positive
 1265 (AP) and Actual Negative (AN) represent human judgments of correctness and incorrectness, respectively,
 1266 while Test Positive and Test Negative indicate the LLM grader’s corresponding evaluations.

1267

1268

The results, shown in Table 7, demonstrate a strong alignment between human preference and LLM-based
 judgments across all evaluated models. For instance, in the case of Qwen2.5-VL’s responses, when humans

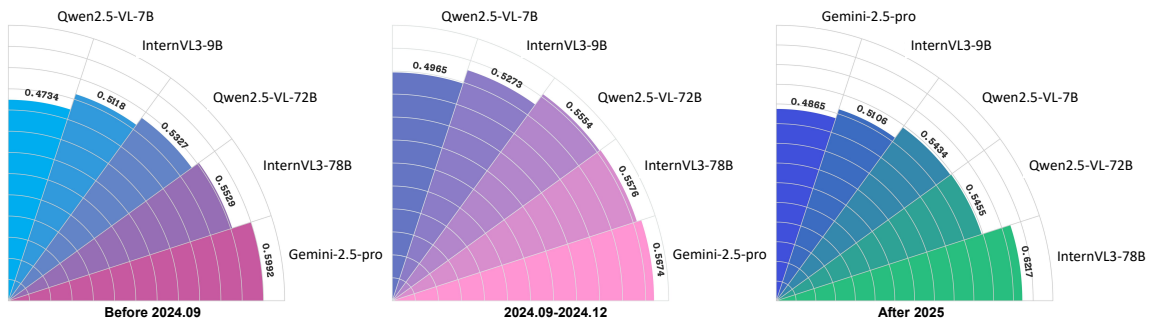


Figure 10: Model accuracy on SKI task across temporal split.

labeled an answer as correct (AP), the LLM grader also marked it as correct 97.13% of the time. Similarly, when humans judged an answer as incorrect (AN), the LLM grader agreed 96.14% of the time. Comparable trends are observed for InternVL3 and Gemini2.5-pro, though with slightly larger gaps in negative cases. These findings suggest that the LLM grader provides a highly reliable approximation of human judgment, especially for positive cases. Incorporating human validation thus not only confirms the feasibility of using LLMs as evaluators but also highlights their potential to scale evaluation consistently across large datasets while retaining strong alignment with expert human preference.

Method	Qwen2.5-VL		InternVL3		Gemini2.5-pro	
	AP	AN	AP	AN	AP	AN
Test Positive	97.13%	2.87%	94.70%	5.30%	93.65%	6.35%
Test Negative	3.86%	96.14%	7.77%	92.23%	11.41%	88.59%

Table 7: Human evaluation for the models’ responses.

A.12 TEMPORAL GENERALIZATION PERFORMANCE

We visualize the accuracy of the best few models on data from different time periods in Figure 10, including Qwen2.5-VL (7B/72B), InternVL3 (9B/78B), and Gemini-2.5-Pro. Notably, models released after late 2024, such as InternVL3-78B and Qwen2.5-VL-72B, consistently outperform Gemini-2.5-pro on contemporary data, although their overall performance lower than Gemini-2.5-pro. The experimental results further supporting the observation that newer models tend to generalize better to new data distributions. This trend underscores the impact of scaling, instruction tuning, and exposure to temporally aligned data in enhancing multimodal reasoning performance.

A.13 MORE ON SMEC VS. BASELINE METHODS

To further highlight the advantage of our proposed SMEC framework, we provide additional qualitative comparisons against baseline methods, including direct inference and ChatGPT-style single-pass reasoning. Figure 11 showcases representative challenging samples drawn from `Lens`, where baseline models tend to produce either incomplete or overconfident predictions.

In these cases, ChatGPT and other baselines often failed for two recurring reasons:

1316 **Over-Reliance on Surface Cues.** Baselines typically produced answers anchored on the most salient visual
 1317 elements, neglecting contextual or relational signals. For instance, when asked to infer spatial constraints or
 1318 traffic rules, ChatGPT tended to extrapolate directly from textual OCR cues, leading to plausible but incorrect
 1319 answers.

1320 **Lack of Internal Deliberation.** Without multi-perspective reasoning, baselines converged prematurely on a
 1321 single hypothesis. This often caused brittle errors in scenarios requiring integration of textual, spatial, and
 1322 commonsense evidence.

1324 By contrast, SMEC decomposed the problem into multiple role-specific perspectives, such as a scene analyst,
 1325 a spatial reasoner, and a cultural or commonsense expert. These experts generated partially overlapping but
 1326 complementary hypotheses, which were then screened for redundancy and synthesized into a consensus. In
 1327 the traffic-sign example shown in Figure 11, SMEC correctly filtered out spurious cues and converged on the
 1328 right driving instruction, whereas ChatGPT remained uncertain or hallucinated unsupported details. Across
 1329 difficult samples, two consistent patterns emerged:

1330 **Error Correction through Redundancy Filtering.** Even when some experts produced misleading interpre-
 1331 tations, SMEC’s screening stage effectively down-weighted unreliable reasoning chains, preventing error
 1332 propagation.

1333 **Multi-Step Enrichment.** Iterative expert collaboration yielded richer reasoning trajectories, allowing the
 1334 framework to exploit synergies between visual grounding, OCR, and commonsense inference. This process
 1335 systematically improved robustness to ambiguous or noisy inputs.

1336 Taken together, these results suggest that SMEC is not merely a test-time ensemble but a principled framework
 1337 that encourages internal debate within a single model. Unlike single-pass inference, SMEC operationalizes a
 1338 language-native form of deliberation, enabling models to approximate the dynamics of human expert panels.
 1339 As Figure 11 illustrates, this mechanism directly translates into more accurate and interpretable reasoning on
 1340 complex multimodal questions.

1341 1342 1343 A.14 LIMITATIONS

1344 While `Lens` offers broad task coverage and a unified evaluation setting, it currently focuses on static
 1345 images and short-form reasoning. Real-world applications may require multimodal reasoning over temporal
 1346 sequences or long-form narratives, which are beyond the scope of this version. Additionally, SMEC relies on
 1347 prompt-based expert simulation, which, though flexible, may introduce redundancy or sensitivity to prompt
 1348 phrasing.

1349 1350 1351 1352 1353 A.15 PROMPTS FOR SYNERGY TESTING

1354 1355 1356 1357 Prompt p_s with OCR question-answer pairs as context

1358 $\{question\ from\ SKI\}$

1359 You can use the following facts to help you answer this question. Please note that they may not be
 1360 relevant to the question. Here are some factual questions and answers about this picture:

1361 $\{question\ from\ OCR\}: \{answer\ from\ OCR\}$

1363
1364
1365
1366
1367
1368
1369
1370
1371
1372
1373
1374
1375
1376
1377
1378
1379
1380
1381
1382
1383
1384
1385
1386
1387
1388
1389
1390
1391
1392
1393
1394
1395
1396
1397
1398
1399
1400
1401
1402
1403
1404
1405
1406
1407
1408
1409

Q: Is my floor the 2nd floor?



SMEC Answer:
Based on the information in the image and a detailed analysis of the signage, your current location is indeed **3rd Floor**. Here's the complete answer and additional explanation:

- Analysis of key information in the image:**
 - Signage on the left:**
 - 5th Floor: Balai Perlepasan (Departure Hall). This is where passengers board their planes.
 - 4th Floor: Pejabat Penyelegaran (Airline Offices). This is where airline staff work.
 - 3rd Floor: Balai Ketibaan (Arrival Hall). This is where passengers go after deplaning.
 - 2nd Floor: Hotel Sama-Sama (Hotel), Medan Kareta C & D (Parking Lot), Medan Sejera (Food Garden). These are areas offering accommodation, parking, and dining options.
 - 1st Floor: Hailing (Parking Area) and Free Shuttle to Kuala Lumpur. This is the parking and shuttle service area.
 - Signage on the Right:**
 - The sign on the right clearly states "Level 3" and has an arrow pointing in a direction. This immediately indicates that you are on the **3rd Floor**.
 - The sign on the right also mentions "Stesen Bas - Terminal 2 / Destinasi Lain" (Bus Station - Terminal 2 / Other Destinations), further confirming that you are on the **3rd Floor**, as this area often houses transportation transfers.
 - Ground Level Signage:**
 - There are yellow signs on the ground that say "E-HAILING" indicating that this is a taxi or ride-hailing waiting area. These areas are usually located on lower floors (such as the 1st or 2nd floor), but the signs here are likely to help passengers quickly find the relevant services.
 - Pedestrians and Luggage:**
 - The image shows several pedestrians dragging suitcases, further confirming that you are near the **Arrival Hall**, as this is where passengers go after deplaning.

Direct Answer (from ChatGPT):
From the signs in your photo, you are currently on Level 2.
I can see the directory on the left which shows:
Level 5: Departure Hall
Level 4: Arrival Hall
Level 2: Bus station, food garden, car parks, hotel, etc
And the purple signage above indicates "Aras Level 2."
 So yes, your floor is the 2nd floor (Level 2 / Aras 2).

Final answer: \boxed{3}

Q: Determine which country this restaurant is located in.



SMEC Answer:
Based on clues in the image and detailed expert analysis, we can draw the following conclusions:

- Key Clue Analysis:**
 - Language Sign:** The sign on the door, "KELUAR," means "exit" in Malay. Malay is primarily spoken in Malaysia, Brunei, and parts of Indonesia. However, Malaysia has the most developed café culture among these countries, and the decor and ambient features in the image are highly consistent with Malaysian café culture.
 - Decorative Style:** The restaurant's interior features wooden tables and chairs, industrial-style pendant lights, and retro posters, creating a modern and unique yet warm design. This style is popular in Southeast Asian countries, particularly Malaysia and Singapore, particularly among independent cafés and small restaurants in cities.
 - Environmental Features:** The restaurant's interior features large windows, allowing for ample natural light and creating a bright and comfortable atmosphere. This design is common in Southeast Asian countries, particularly Malaysia, due to the warm and humid climates in these regions, where interior design often prioritizes natural light. Additionally, the restaurant's furniture (such as wooden tables and chairs with wrought iron frames) and air conditioning (wall-mounted) are consistent with Malaysia's climate and design practices.
- Eliminating Other Possibilities:**
Brunei: Although Brunei also speaks Malay, its smaller land area and sparse population don't allow for a more developed café culture than Malaysia. Therefore, Brunei is less likely. Indonesia: Indonesia's primary official language is Indonesian, not Malay. While Malay may be spoken in some areas, Indonesian café culture tends to be more modern and international, which doesn't align with the retro, industrial-style design in the image.
- Additional Expert Analysis:**
Based on analysis by experts on Southeast Asian café culture and design trends, the restaurant's wooden tables and chairs, industrial-style pendant lights, and retro posters align with café design trends in Malaysia and other Southeast Asian countries, particularly Malaysia's multiculturalism and its blend of modern and retro styles.
- Spatial Layout and Atmosphere:** The restaurant's open layout, ample use of natural light, and spacious design perfectly complement the climate and culture of Southeast Asia, particularly Malaysia.
- Cultural Fusion:** The restaurant's design embodies a blend of Eastern and Western elements, while respecting local culture, a typical characteristic of Malaysian cafés.
- Comparison with Other Southeast Asian Countries:** Singaporean cafés are generally more modern and international in design, while Thai cafés may incorporate Buddhist elements and tropical themes. This restaurant's style is more closely aligned with Malaysian characteristics.
- Final Conclusion:**
Based on the above analysis, this restaurant is most likely located in Malaysia. The Malay sign "KELUAR" is a key clue, and the restaurant's decor and surroundings are also highly consistent with Malaysian café culture.

Final answer: \boxed{Malaysia}

Figure 11: Comparison of our method and ChatGPT on some difficult examples.

1410
1411

A.16 PROMPTS OF SELF-DRIVEN MULTI-EXPERT COLLABORATIVE FRAMEWORK

1412
1413Meta Generation Prompt p_g

1414

{question}

1415

Here are your answers and those of some experts:

1416

{answer}

1417

Now you can create and work with multiple experts to improve your answer. So, please describe in as much detail as possible the different skills and focus you need from each expert.

1418

We will provide each expert with the same information and queries. Each expert should have his or her own specialization covering perception, understanding and reasoning, etc., so you can assign only one subtask to each expert to ensure a more refined answer. We will relay their responses to you in turn so that you can reorganize them into better answers. Please note that descriptions should be in the second person, e.g. You are XXX.

1419

These are the descriptions of the experts you have previously created for this task:

1420

{description}

1421

Therefore, do not create the same experts as above over and over again.

1422

Now you can create a description for the new expert (please note that you can only describe one, not more than one at the same time):

1423

1424
1425Inspection Prompt p_c

1426

{question}

1427

We hired multiple experts to answer this question. Below is a second person description of the experts we hired: {existing description}

1428

We are now hiring a new expert to help better provide the information needed for the question as well as respond to user queries. Here is a second person description of the new expert: {description}

1429

Since there is an additional cost to hiring a new Expert, please evaluate the new Expert based on the following two criteria to decide whether or not to retain them.

1430

1. based on the new Expert's description, determine if they can effectively assist in answering the user's question or provide the information needed for the question.

1431

2. the new expert is not a duplicate of any existing expert.

1432

The new expert must meet both of these criteria. If either criterion is not met, they should be discarded.

1433

If retaining, please reply 'Retain'. If discarded, please reply: 'Discard'.

1434

1435

Collaboration Prompt p_c

1436

{question} These are you and some experts' answer: {answer}

1437

The description of the experts you invited are: {description}

1438

Now, you can refine your answer based on the answer and additional information they provided to better answer the question. Keep in mind that the experts' answer and additional information may not be correct, so decide carefully whether to accept his answer or stick to your original one.

1439

Revised answer:

1440

1441

A.17 THE USE OF LARGE LANGUAGE MODELS (LLMs)

1442

We have not used Large Language Models (LLMs) for our paper writing.

1443